Switching Notes
Note 5
June 1969

A Laser-Triggered Switch Employing Solid Dielectrics

Lt Daniel M. Strickland
Air Force Institute of Technology
and
Air Force Weapons Laboratory

Abstract

A focused, Q-spoiled laser was used to induce electrical breakdown of the solid dielectric between two charged electrodes. The effect of the following parameters on the breakdown delay was studied: laser focal point, applied voltage (30-85 KV), charging polarity, laser power (20-90 MW), dielectric thickness (10-20 mils), and dielectric type (Lexan and Teflon FEP). Delay times as short as 3 nsec, with 1 nsec jitter, were recorded. Graded dielectrics were found to decrease switch closure time through the formation of multiple breakdown channels. Observed results seem consistent with the avalanche-streamer theory of solid breakdown.

Contents

Contents

List of Figures

List of Important Symbols

t_d	time delay between the arrival of the laser pulse at the gap and complete breakdown of the gap
t_L	total length of laser pulse duration
α	ionization coefficient
γ	recombination coefficient
ν_o	rate of electron production from the cathode
θ	rate of ionization in plasma by laser interaction
d	sample thickness
ΔS	cross-sectional area of laser-induced plasma
N_Σ	number of positive ions required for streamer formation
V_t	voltage at which transition from low delay region to high delay region occurs

A LASER-TRIGGERED SWITCH EMPLOYING SOLID DIELECTRICS

I. INTRODUCTION

Statement of Problem

The technique of using a focused, giant-pulse laser to break down the dielectric between charged electrodes, thereby initiating an electrical discharge across the gap, is called laser-triggered switching (LTS). LTS was first reported by Pendleton and Guenther who used gas dielectrics and kilovolt potentials (Ref. 28). Guenther and Bettis have since extended this technique into the megavolt range (Ref. 15).

This study represents an attempt to determine the suitability of solid dielectrics for use in laser-triggered switching. Solids are interesting because of their high dielectric strengths and their ability to pass large amounts of charge with minimum electrode erosion. These characteristics enable switches which have high voltage holdoffs at relatively small gap spacings to be constructed. Small gaps are desired because the impedance of the switch is proportional to the length of the gap. Therefore solid dielectrics provide the possible means for operating high voltage switches with low impedance and fast closure times obtained through laser initiation.

In particular this study involved the determination of the time interval (delay) between the arrival of the laser pulse at the gap and breakdown of the gap. Jitter or average deviation from the mean delay

was also studied as well as the voltage risetime upon gap closure. Switch delay and jitter were studied as a function of applied voltage, electrode polarity, laser power, laser focus, material thickness, and type of material. In addition, graded dielectrics were studied to determine their effect on switch closure time.

Importance of Problem

The USAF nuclear survivability/vulnerability program is a vital part of DOD's effort to maintain the effectiveness of America's defensive and strategic weapons systems. However, because of the ratification of the Limited Test Ban Treaty, atmospheric testing of nuclear weapons systems has been suspended. Consequently, there are only two physical methods available for evaluating the survivability/vulnerability of operational and future weapons systems: underground testing and laboratory simulation.

The environmental and geometrical limitations imposed on underground testing create several disadvantages such as time scale compression, weapon output modification, spurious damage to test objects due to late time effects, difficult sample recovery, and slow testing rate. In addition, the cost of underground testing is very great. However, the suitability of laboratory simulation techniques depends on two factors: (1) whether effects or environments are simulated, and (2) whether whole systems or only components of a system can be tested.

Effects simulation is defined as the process of reproducing a particular response or combination of responses without recourse to the environment that caused them, e.g., a plate slap technique to simulate certain photon effects. Environmental simulation involves actually reproducing part of a weapon output in the laboratory.

The validity of effects simulation is sometimes difficult to analyze. Techniques such as charged particle simulation of photon effects produce averaged rather than actual responses, and accompanying effects such as charge storage can affect target response. In addition, no effect can be simulated unless the interaction of the weapon environment with the test object is adequately understood. Therefore, the logical course is to develop simulation devices which can produce the appropriate weapon-like environments in the proper time scale and over large areas and volumes. There are three important factors in producing a weapon-like output which can benefit from the development of laser-triggered switch: (1) Flux Levels, (2) Area of Irradiation, and (3) Temporal Characteristics.

For example, consider gamma ray simulation. The Air Force Weapons Laboratory currently has flash gamma machines which operate at 10 megavolts and employ field emission diodes. Field emission electrons from the cathode are made to impinge on a high Z anode target, producing bremsstrahlung X-rays. Such high energy X-rays are used to simulate the gamma output of a weapon. Let us consider the benefits to the operation of these machines that might be derived from a laser-triggered switch.

Flux Levels. One such machine is designed with a 40-ohm impedance, and since it operates at 10^7 volts, its current output is $\sim 2.5 \times 10^5$ amps and its power output is $\sim 2.5 \times 10^{12}$ watts. This output power produces a gamma yield of about 5×10^3 rad. However, requirements now exist for outputs of 5×10^4 rad which may require powers of 10^{14} watts. To achieve this power level, a machine must be built with a higher current capability, since the voltage is limited

to about 10^7 volts. Above this voltage the (γ,n) cross section becomes large and so many photoneutrons are produced that the test area can become activated. It is therefore necessary to reduce the generator impedance to 1 ohm so that currents of 10^7 amps can be achieved.

Herein lies one problem in building a single 10^{14}-watt machine. Voltage holdoffs of 10^7 volts require large separations between conductors while impedances of 1 ohm require small separations between conductors. One way to bypass this difficulty is to build ten 10-ohm machines and arrange them in parallel to a 1-ohm transducer.

The key to accomplishing this task lies in the switch which is used to dump the stored energy into the transducer. All 10 machines must be switched with a simultaneity of about 10 percent of the desired risetime, which is on the order of 10 nsec. Nonsimultaneity in switching increases the risetime of the gamma output from the transducer and decreases its resemblance to the true output of a weapon. In addition, the impedance mismatch at the transducer would cause reflections which could result in high-voltage damage to the machines.

Multiple-gap laser-triggered switching with low nanosecond jitter such as that reported by Guenther and Bettis (Ref. 16), could reliably switch these machines in the required time interval. A solid dielectric LTS with such reliability would be even better because of its higher voltage holdoff capability and smaller switch impedance.

Area of Irradiation. The simultaneous switching of many machines also provides the means for testing system size devices by increasing the area of irradiation. It is not possible at present to increase the size of the individual machines beyond that size which can be shipped by rail.

Temporal Characteristics. Since many outputs of a nuclear weapon last for a very short time ($\sim 10^{-7}$ sec), the energy stored must be dumped into the transducer in comparable times in order to simulate the weapon output. If the switch were a perfect one (zero impedance) which closed instantaneously, then the risetime of the current into the transducer would depend only upon the impedance of the generator. However, the switch inductance and resistance increase the current risetime. In addition, the impedance of the switch results in a power loss to the transducer which reduces the overall efficiency of the simulator. For instance, if a 1-ohm switch were used with a 1-ohm generator, half the energy would be dissipated in the switch. But if the switch impedance were reduced to one-tenth ohm, then the energy loss would be reduced to 10 percent. It is therefore desirable to make the switch impedance as low as possible.

Since the impedance is proportional to switch gap spacing, solid dielectrics are advantageous for this use. They have generally higher dielectric strengths than gases or liquids and can therefore hold off high voltages with lower gap spacings. Another way to reduce switch impedance is to trigger multiple breakdown channels in the gap. This decreases both switch inductance and resistance. Multiple-channel laser triggering in solids can potentially be achieved in two ways. One way is to physically separate the triggering laser pulse into two or more beams as Guenther did (Ref. 13). The other way is to use compound or graded dielectrics to initiate multiple channels with one laser beam. This method consists of putting a thin piece of metal foil between two pieces of solid dielectric and firing the laser into

the foil. As will be shown later in this report, the resulting effect is the initiation of multiple breakdown channels around the perimeter of the foil due to field enhancement.

Survey of Previous Studies

The first paper on LTS was published by Pendleton and Guenther (Ref. 28). They focused a Q-switched ruby laser of 25 to 80 MW perpendicular to the axis of a sphere-sphere gap and studied switching characteristics as functions of laser power, dielectric gas, gas pressure, gap spacing, electric field, and focal point location. Delays as low as 10 nsec were achieved in SF_6 at atmospheric pressure when the laser was focused on the high voltage electrode. Similar results were reported by Barbini (Ref. 2).

Lower delays and jitter were reported by Deutsch (Ref. 10). A coaxial spark gap (4 to 10 mm) with various gas dielectrics charged as high as 120 KV was triggered with 1 nsec delay and 1 nsec standard deviation.

The use of high vacuum as a switch dielectric for LTS was investigated by Clark et al. (Ref. 7). Delays in the low microsecond range were achieved with the use of a 1-MW Q-switched ruby laser triggering a 300-KV gap. Similar results were achieved with a pulsed nitrogen laser at repetition rates of 5 pps.

High repetition rate switching in a time regime of more interest to this study was reported by Guenther and McKnight (Ref. 17). A low-energy, high-brightness YAG laser was used to switch a gas gap at 50 pps with less than 1 nsec jitter.

To extend LTS into the megavolt regime, Guenther and Bettis (Ref. 15) used a ruby laser of 100 to 250 MW to trigger a 50-ohm coaxial

capacitor by firing the laser along the interelectrode axis. Delays of 2 nsec with 0.2 nsec jitter were reported.

Interesting results in the areas of multigap switching and multichannel switching were achieved by Guenther et al. Four gas gaps were fired at 50 pps within 0.1 nsec of each other using a YAG laser (Ref. 16), and a factor of 2 reduction in current risetime was obtained by the simultaneous initiation of two breakdown channels in a single switch (Ref. 13).

In addition to the studies mentioned so far, which used either gas or vacuum-filled switches, one other dielectric has been investigated for use in LTS. Marolda (Ref. 25) used transformer oil in a sphere-sphere gap with spacing of 0.365 cm and studied two triggering configurations. Microsecond delays were measured when the laser was focused perpendicular to the electrode axis but decreased to as low as 30 nsec when the laser was focused along the interelectrode axis.

II. THEORY

In general, solid breakdown theories deal with the work done on conduction electrons by an applied field. These electrons transfer some of their energy to the matrix (or lattice) through collisions and thus raise its temperature. Breakdown occurs when the matrix temperature T_m reaches some critical value T_m'. The various theories of dielectric breakdown differ primarily in the conditions which govern the energy transfer from the field to the matrix via the conduction electrons. These theories may be broadly classed as either "thermal" or "intrinsic" (Ref. 32).

For "thermal" breakdown it is assumed that the electrical conductivity is increasingly dependent upon T_m and thus depends only implicitly on the applied field. It is therefore a macroscopic theory involving the generation and transfer of heat in the classical sense.

However, "intrinsic" breakdown theories assume that the electron distribution itself depends directly on the applied field. Thus the conductivity and rate at which the electrons supply energy to the matrix are explicit functions of the applied field. The problem is, therefore, a microscopic one involving the calculation of the number and density of conduction electrons and their energy distribution and momentum under an applied field. Intrinsic breakdown itself may further be divided into two types: "collective" and "avalanche."

"Collective" breakdown theories assume that the density of conduction electrons increases due to internal field emission. After the electron density reaches a certain value, the collisions between

electrons determine their energy distribution. This distribution is Maxwellian with a characteristic electron temperature T_e which depends upon the applied field. If the applied field is greater than a certain critical value, T_e increases without limit until collective breakdown occurs.

The "avalanche" breakdown theory of solids is similar to avalanche theories for gases. Electrons are accelerated by the field and gain sufficient energy to liberate more electrons through collisional ionization from bound states in the matrix. However, the calculation of the electron distribution in avalanche breakdown is more complicated than that for collective breakdown. This is because both ionizing collisions and recombination collisions must be included in the distribution calculations.

A further manifestation of the avalanche theory is the postulation of a photo-ionization process, sometimes referred to as the "streamer theory." The present consensus seems to indicate that for solids at room temperature and above the avalanche-streamer theory best fits experimental results (Refs. 21, 22, 27, and 32 through 36). On this basis it was decided that a detailed discussion of the avalanche-streamer theory would be of more value to this study than a superficial discussion of both collective and avalanche-streamer theories. In addition, experimental results supporting the latter theory will be discussed.

The results of this study will be interpreted in light of the avalanche-streamer theory in a later section. However, it is emphasized that no attempt will be made to exclude explanations of these results on the basis of other theories. The current understanding of

solid breakdown processes is still too incomplete to allow an exclusive approach to the analysis of experimental data.

Avalanche-Streamer Theory

To begin a qualitative discussion of avalanche breakdown in solids, let us first postulate that an electron is released from the cathode of a charged spark gap. This electron may be released by means of cosmic or ultraviolet radiation, thermionic emission, field emission, or some other initiation process. As soon as the electron is released, it will begin to drift toward the anode with a velocity and a path characteristic of the applied field and the particular solid dielectric.

Several things can happen to this electron in its progress toward the anode. One possibility is that it will suffer only elastic collisions with the solid matrix and will merely be scattered randomly about through the gap with its net motion still in the direction of the applied field. Another possibility is that it will suffer an inelastic collision resulting in capture by the matrix or recombination with a positive ion. In this case the electron is removed from the gap with the resulting production of a photon which may in turn ionize an atom in the dielectric or even release a charged particle from an electrode. A third major possibility is that the electron will gain enough energy from the applied field to suffer an ionizing collision resulting in the release of another electron. This new electron in its transit toward the anode may interact as did the original electron.

As it turns out, for insulating solids at fields below those required for breakdown, the most likely process is the second one mentioned. That is, if an electron does happen to be emitted from the cathode or even from the bulk of the dielectric, it will probably be

captured. For fields near breakdown a few electrons may acquire enough energy from the field to either avoid recombination or to release more electrons through collisional ionization so that a small (10^{-14} amp) (Ref. 24) steady-state current may be set up. Over long periods of time (minutes-years) this current may cause enough damage through heating and chemical deterioration of the dielectric to cause dielectric breakdown. However, in the time regime of interest to this study ($< 10^{-5}$ sec) these small prebreakdown currents do essentially no damage to the dielectric. At fields sufficient for breakdown of the dielectric, the situation is different. An individual electron can gain sufficient energy from the field to multiply through collisional ionization and spread out, due to diffusion, into a conical-shaped path of ionization which propagates toward the anode. Because of the "snowballing" nature of its growth, this process is appropriately called an avalanche.

In the process of its growth in the gap, an avalanche can damage the dielectric in two major ways: (1) through heating due to electron-matrix energy exchanges and (2) through disruption of the matrix structure from ionizing collisions. Depending upon the field and the nature of the dielectric, a single avalanche may reach a sufficient size to cause enough damage to break down the dielectric. If one avalanche does not cause breakdown then further avalanches may form until the dielectric is damaged sufficiently for breakdown to occur.

Due to the complex nature of this process in solids, no satisfactory expressions have yet been developed to predict the behavior of a solid dielectric under high electrical stress. In fact, it has been necessary to propose another distinct but avalanche-related mechanism

to explain certain characteristics of solid breakdown. This is the streamer mechanism and is analogous to the mechanism of the same name in gas breakdown.

The streamer mechanism in gases was first proposed in 1936 by Raether and Flegler (Ref. 24). The explanation of the process goes as follows: First an avalanche crosses to midgap or near the anode. At a certain point in the growth of this avalanche the positive ion densities in the trailing portion of the avalanche (cathode end) become sufficient to produce local fields which distort and augment the applied field. Then recombination photons emitted from the positive space charge cause photoelectric ionization in two regions: (1) between the positive space charge and the cathode and (2) between the negative avalanche head and the anode. The photoelectrons produced in these localized, intense field regions produce new avalanches and rapidly spread the discharge toward the anode and toward the cathode.

It is also possible that a single avalanche will not reach a sufficient size to form the positive space charge density required for streamer formation. In this case it might require several or even many avalanches to form. The space charge formed by each successive avalanche would then add to the space charge formed by preceding avalanches until the cumulative space charge was sufficient to form streamers.

Therefore the question arises as to how one determines whether a particular breakdown event is pure avalanche or whether it is avalanche-streamer. The answer to this question depends upon the dielectric being studied. In gases one simple way to make this determination is to take cloud chamber photographs of the breakdown. The avalanche photographs as an orderly growth of conical ionization

spreading from the cathode toward the anode. If a streamer is formed, it photographs as a filament of ionization which seems to have no distinct point of origin in the gap (Ref. 24).

In a solid dielectric, however, the observation of a streamer process must usually be made indirectly, such as with the use of a voltage cutoff method. This method consists of applying a high voltage to a dielectric for a certain length of time and removing the voltage before the sample has broken down completely. This procedure results in partial breakdown of the solid, the analysis of which yields information about the breakdown process.

Vorobev et al. (Refs. 34, 35) used the cutoff method to test solid dielectrics in a point-plane gap. He found that when the point electrode was positive a definite breakdown channel formed from the anode and propagated toward the cathode. The length of the channel increased as the pulse duration increased until the channel completely bridged the gap and breakdown occurred. However, when the point electrode was negative, the partial breakdown manifested itself, not as a definite channel, but as a barely visible region of disturbance.

The results of Vorobev's research point strongly toward an avalanche-streamer mechanism in his observations. The reason for this conclusion is that an electron avalanche cannot propagate from the anode to the cathode, but a streamer can. Therefore, the observed breakdown channel emanating from the point-anode was concluded to be a streamer which was formed in the positive space charge around the anode. This streamer propagated outward (toward the cathode) and was enhanced by avalanches going in the other direction. When the voltage was cut off, the avalanches stopped and the streamer stopped, leaving an incomplete breakdown channel.

For a point-cathode, on the other hand, Vorobev concluded that the avalanches were hindered by the formation of a positive space charge around the cathode. In other words, electrons emitted from the cathode traveled through a field region which encouraged recombination rather than multiplication. As a result, when the voltage was cut off before breakdown occurred, no streamer had formed so that the only breakdown damage observed was the small amount done by the weak avalanches.

Additionally, it was found that a negative point configuration held off higher voltages than a positive point, and from the previous discussion, this observation seems reasonable. The conclusion therefore is that a streamer mechanism is apparent if the breakdown process is more rapid when initiated from the anode than when it is initiated from the cathode.

Laser-Induced Breakdown

In order to obtain at least a semiqualitative understanding of how a laser can initiate electrical breakdown of solid dielectrics, let us assume that breakdown occurs through an avalanche-streamer process. Further, let us assume that streamers will form and breakdown will occur after a specific number of positive ions, N_Σ, have accumulated at the anode. The time required for breakdown to occur will then depend primarily upon the time to accumulate N_Σ (the streamer transit time being negligible) (Ref. 15).

The buildup of N_Σ depends upon three processes: (1) generation through laser ionization, (2) generation through electronic avalanches, and (3) loss through recombination.

The first process involves both initiation and buildup. As the focused laser beam first impinges on the electrode, a metallic plasma is generated from the electrode surface and some additional plasma is generated in the dielectric itself. The formation of such plasmas by a focused laser is well documented (Refs. 7 through 9, 11, 18 through 20, 26, 29 through 31, and 38). Once the plasma is initiated, it continues to absorb the incident laser energy through inverse bremsstrahlung interactions with plasma electrons. These energetic electrons then ionize neutral atoms and the degree of ionization increases.

The ion production term from the laser-plasma interaction is given by (adapted from reference 29):

$$dN_1 = N_o \theta \, e^{t\theta} \, dt \qquad (1)$$

where

N_1 = number of ionizations which result from laser-plasma interaction

N_o = initial number of electrons in plasma

θ = number of electrons produced per second

The ion production term from electronic avalanches may be expressed as (Ref. 33):

$$dN_2 = \nu_o \, \Delta S \, 2^{\alpha d} \, dt \qquad (2)$$

where

N_2 = number of ions produced in head of avalanche

ν_o = electron flux from cathode (electrons/cm^2-sec)

ΔS = cross-sectional area of plasma

α = ionization coefficient of dielectric (ionizing collisions per unit path)

d = thickness of specimen

The third term, a loss due to recombination, is given by (Ref. 33):

$$dN_3 = -\gamma N^2 \, dt \tag{3}$$

where

N_3 = number of ions which recombine

γ = recombination coefficient (recombinations/sec-electron)

N = number of ions in plasma

So the incremental buildup of N_Σ is given by:

$$dN_\Sigma = dN_1 + dN_2 + dN_3$$

$$= N_o \theta \, e^{\theta t} \, dt + \nu_o \, \Delta S \, 2^{\alpha d} \, dt - \gamma N^2 \, dt \tag{4}$$

Let

$$A_1 = N_o \theta \, e^{\theta t} \tag{5}$$

and

$$A_2 = \nu_o \, \Delta S \, 2^{\alpha d} \tag{6}$$

For simplicity in the derivation to follow, it will be assumed that A_1 and A_2 remain constant throughout the space charge buildup. This assumption is not true for several reasons, the most obvious of which is that A_1 increases exponentially with time. The second reason is that A_2 increases with plasma buildup: (1) ΔS increases with plasma size, (2) plasma photons cause photoelectric emission from the cathode and increase ν_o, and (3) α increases with applied field and therefore increases as the space charge builds up. However, the increase of A_1 and A_2 may be diminished to some extent by a decrease in θ as the plasma expands. Such expansion is quite rapid because of the high particle energies present in the plasma.

The resultant effect, however, is probably still an increase of A_1 and A_2. The justification for making the gross assumption that these terms are constant is that first it allows us to derive a simple

analytical expression for t_d (time to breakdown by streamer formation), and second, any increase in A_1 and A_2 will only serve to enhance the ability of the laser to initiate breakdown.

Using equations (5) and (6), we can write equation (4) as:

$$dN_\Sigma \approx (A_1 + A_2)\, dt - \gamma\, N_\Sigma^2\, dt \qquad (7)$$

Separating variables and integrating from $t = 0$ to $t = t_d$ yields:

$$N_\Sigma \approx \sqrt{\frac{A_1+A_2}{\gamma}}\ \frac{\exp\left(2\sqrt{\gamma(A_1+A_2)}\ t_d\right) - 1}{\exp\left(2\sqrt{\gamma(A_1+A_2)}\ t_d\right) + 1} \qquad (8)$$

Rearranging and solving for t_d yields:

$$t_d \approx \frac{1}{2\sqrt{\gamma(A_1+A_2)}}\ \ell n \left[\frac{\sqrt{\frac{A_1+A_2}{\gamma\, N_\Sigma^2}} + 1}{\sqrt{\frac{A_1+A_2}{\gamma\, N_\Sigma^2}} - 1}\right] \qquad (9)$$

This equation shows how a laser can initiate breakdown in an under-volted solid where the ion production rate equals the ion recombination rate. Before the laser arrives at the electrode, $A_1 = 0$ and $A_2 = \gamma\, N_\Sigma^2$, yielding $t_d = \infty$. However, when the laser is focused in the gap, the laser production term, A_1, becomes greater than zero, making $A_1 + A_2 > \gamma\, N_\Sigma^2$ and reducing t_d to a finite value. As mentioned previously, even though A_1 and A_2 increase as the plasma builds up, they only serve to enhance the effect of the laser in breaking down the dielectric.

It should be noted that this analysis is not meant to be quantitative. A more detailed treatment would require the inclusion of time-dependent expressions for A_1 and A_2. However, since values for

ν_o, α, γ, and θ are not known, a rigorous treatment is not warranted at present. The usefulness of equation (9) is that it presents a qualitative, lower-limit explanation of laser-induced, electrical breakdown of solids. It is also qualitatively consistent with the results of this study, as will be shown later.

III. EXPERIMENTAL

The experimental apparatus used to study laser-triggered switching in solid dielectrics is shown schematically in Figure 1. The apparatus consisted of three main functional units: (1) the switch tank, (2) the laser system, and (3) the diagnostic equipment.

Switch Tank

The switch tank (Figures 2, 3) served the three-fold purpose of holding the samples to be tested, focusing the laser beam on the electrodes and applying a DC field to the sample. The tank was a 50-ohm impedance coaxial aluminum cylinder, 7.5 inches I.D. and 18 inches long, which held the focusing lenses and switch electrodes. A 12-inch long, 50-ohm constant impedance tapered line of sheet metal was attached to the end opposite the lenses and was connected to a 14-foot length of 50-ohm RG/17A coaxial cable. The end of the cable was connected through a 1-megohm charging resistor to a 0 to 120 KV power supply. The tank and tapered line were filled with transformer oil for insulation.

The capacitances of the elements charged by the power supply were calculated from coaxial geometry formulae using published values of dielectric constants and are tabulated in Table I.

Electrodes. The electrodes (Figure 4) used in this system were the Bruce uniform-field type and were constructed of stainless steel (see Appendix A). The grounded electrode held the beam focusing optics which consisted of a fixed position focusing lens close to the solid

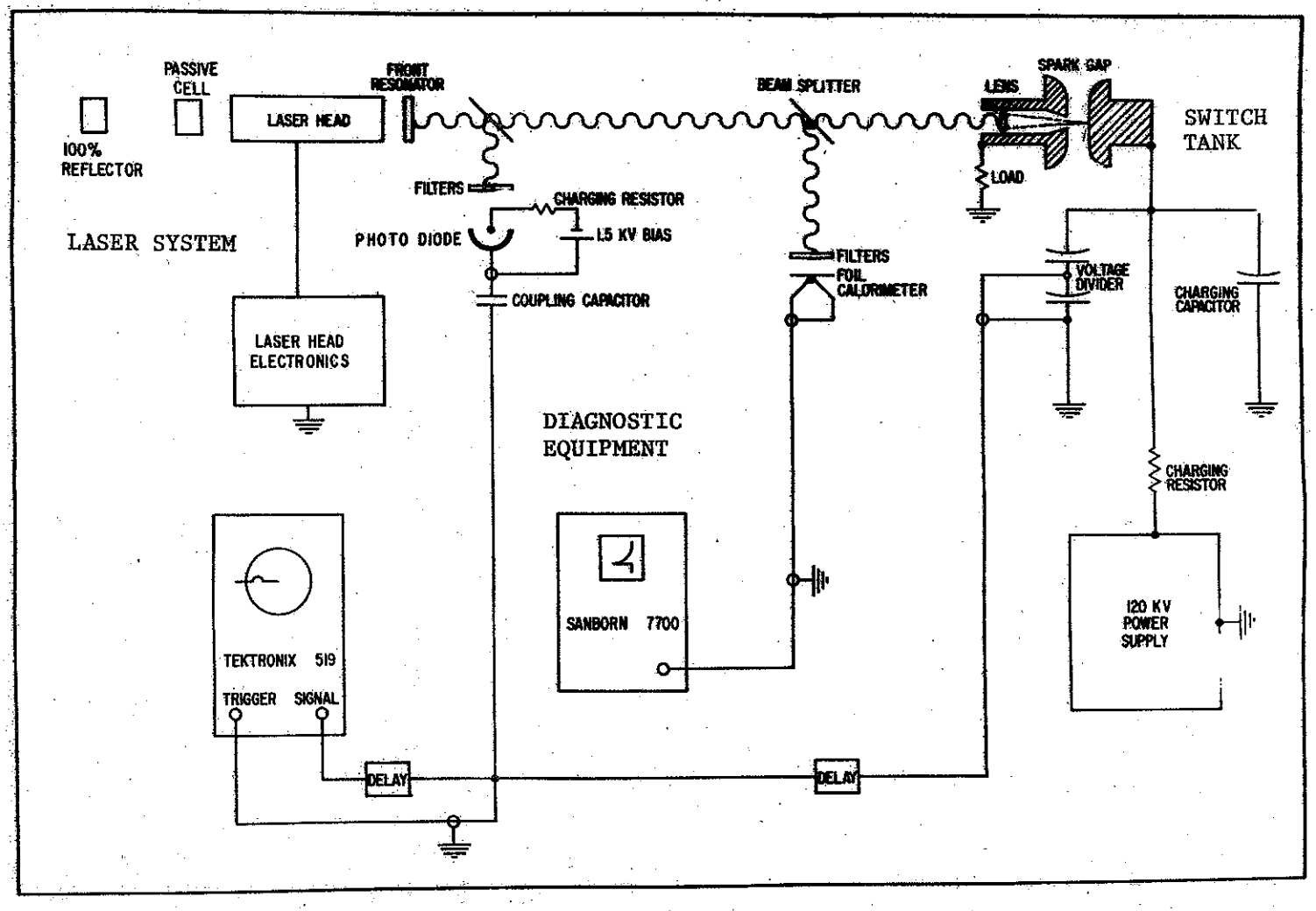

Figure 1. Schematic Diagram of
Laser-Triggered Switching Apparatus

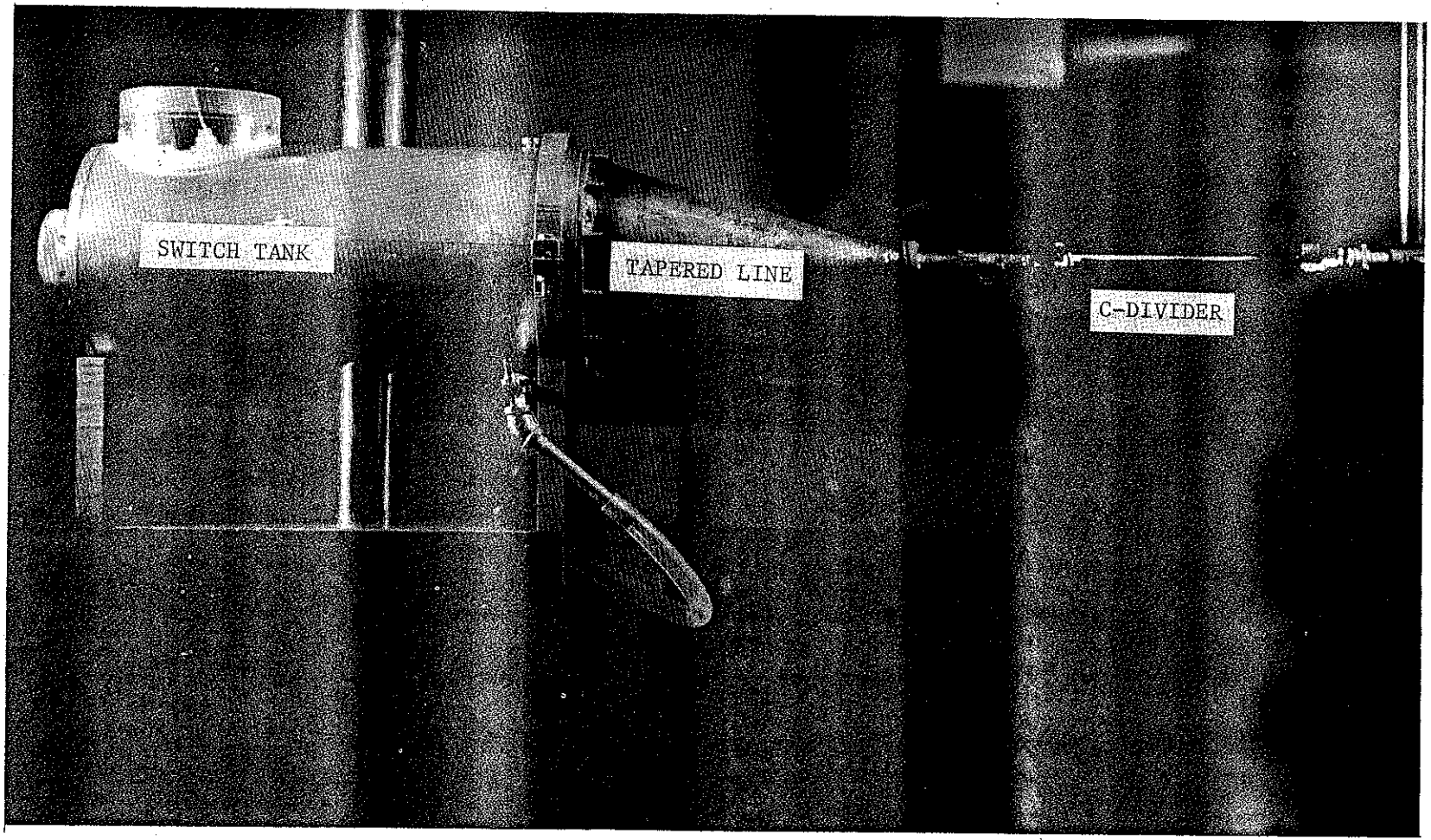

Figure 2. Switch Tank, Tapered Line, and Capacitive Voltage Divider

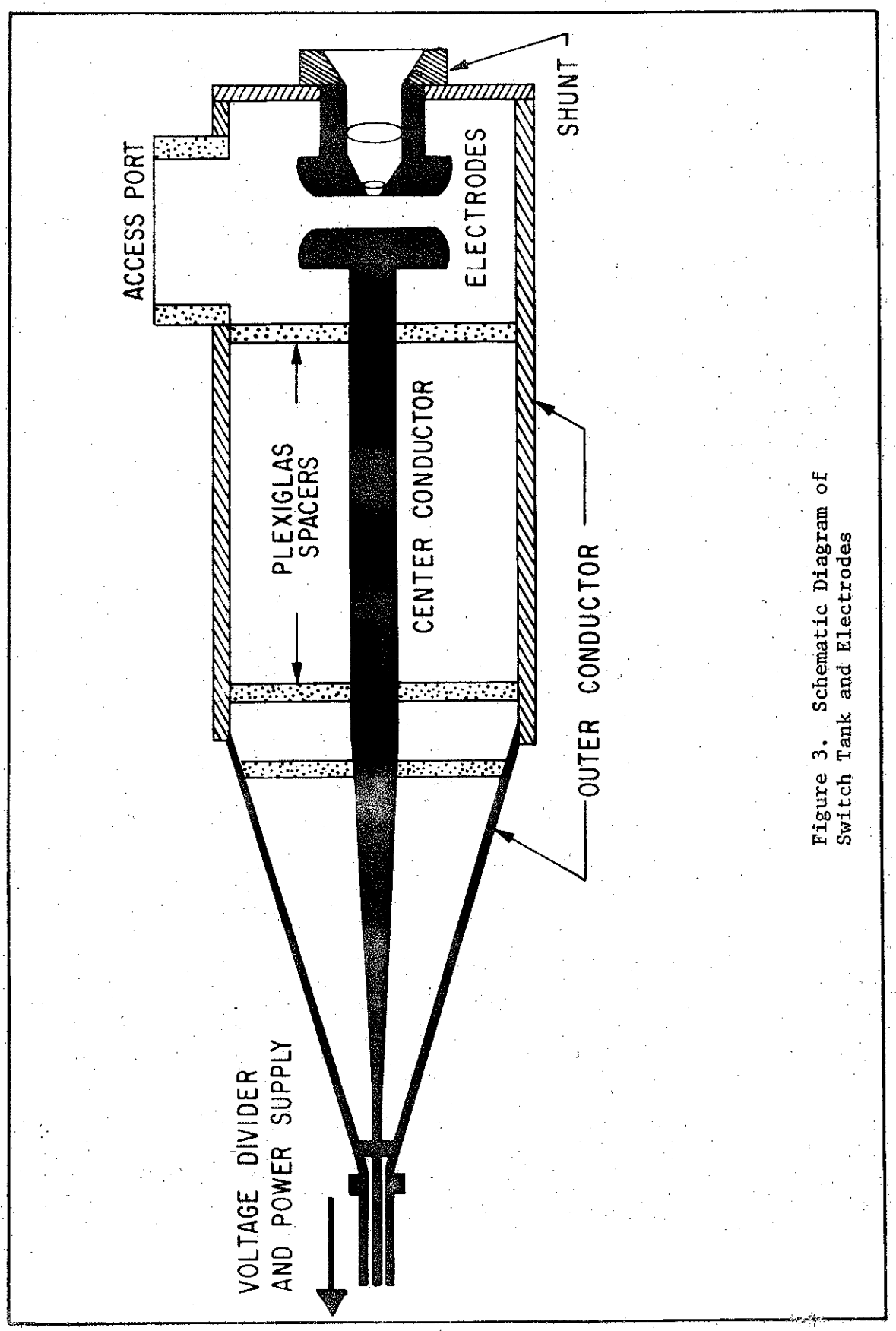

Figure 3. Schematic Diagram of Switch Tank and Electrodes

Table I

CAPACITANCES OF CHARGING ELEMENTS

Element	Capacitance (pf)
14-foot RG/17A	400
Cylinder and tapered line filled with transformer oil	400
Electrodes closed onto 10-mil Lexan sample	500
Total	1300

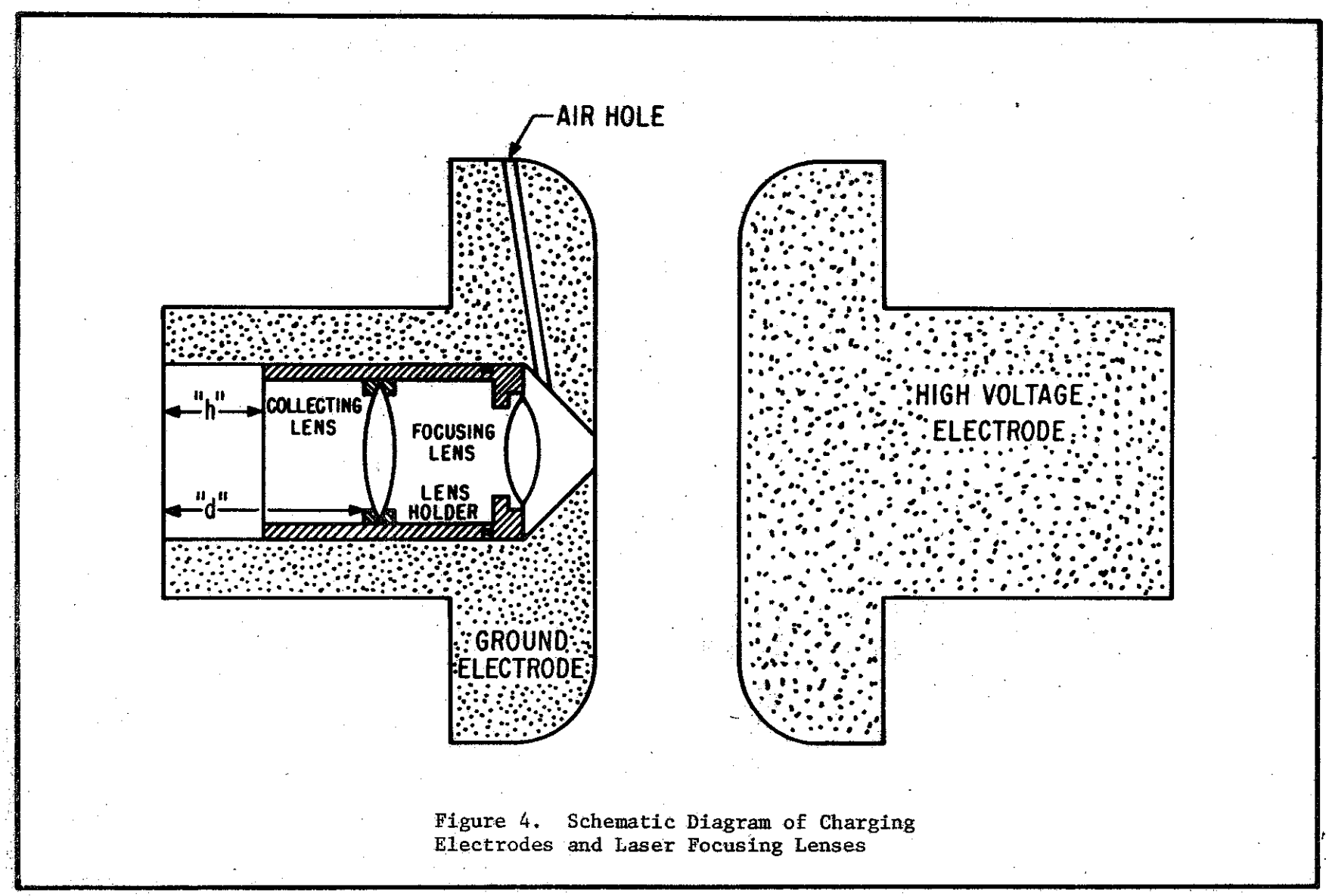

Figure 4. Schematic Diagram of Charging Electrodes and Laser Focusing Lenses

dielectric and a variable position collecting lens mounted into a brass lens holder. The focal lengths in air of the collecting and focusing lenses were 55 mm and 13 mm, respectively.

The space between the two lenses was kept free of oil by an epoxy seal around the focusing lens. An O-ring around the lens holder prevented oil leakage from the chamber. In addition, an air hole was drilled into the ground electrode to provide for removal of air bubbles and contamination which formed after every laser shot. To expel such bubbles and debris, the lens holder was used as a piston and moved in and out several times. It was found that if all air bubbles were not removed from the cavity in front of the focusing lens damage would result to the lens from the laser firing.

Laser System

The laser system used for this research was a Korad model K-2Q ruby laser operated in the giant pulse mode. Q-switching was accomplished by the use of a bleachable dye (cryptocyanine dissolved in methanol) which is discussed in Appendix B.

The optical cavity contained an 0.75-inch diameter, 9.0-inch long ruby rod optically pumped by a single helical Xenon flashlamp. Cavity output reflectors consisted of the flat, uncoated front of the rod ($\sim$ 4 percent) and an 0.125-inch thick sapphire flat ($\sim$35 percent) placed about 10 cm in front of the rod. A 5/8-inch diameter ceramic aperture was placed between the sapphire and the front rod face for two reasons: (1) blow-off of material onto the rod from the aluminum rod holder was reduced, and (2) beam divergence was reduced by the reduction in cavity aspect ratio. The rear cavity reflector was a 100 percent dielectric reflector in front of which was placed the bleachable

dye cell at Brewster's angle. Energy output could be varied continuously from 0 to 4 joules with pulse widths (FWHM) from 30 to 40 nsec. Peak powers used in this study were from 20 to 90 MW.

Diagnostic Equipment

Diagnostic equipment consisted primarily of two types: (1) that which monitored laser characteristics and (2) that which monitored breakdown characteristics.

The laser monitoring equipment served the purposes of recording pulse shape, measuring energy, and providing a time reference. Pulse shape was monitored by an ITT vacuum planar photodiode with a 10-picosec risetime S-20 photocathode. A portion of the laser beam was directed into the diode by a beam-splitter and the signal was fed into a Tektronix 519 oscilloscope which was situated in an RF shielded room. These scopes have risetimes of less than 0.4 nsec and sweep speeds of from 2 nsec/cm to 1000 nsec/cm. Sweep speeds of all scopes were calibrated by the method reported in Appendix C.

Laser energy was measured with a thin-foil calorimeter (foilometer) which is essentially a piece of aluminum foil with a thermocouple attached to the back (Ref. 5). A portion of the laser beam was taken off with a beam-splitter and directed into the foilometer which heated up and produced a thermal-induced emf at the thermocouple. This signal was fed into a Hewlett-Packard model 425AR DC microvoltmeter and recorded on a Sanborn model 7701A heated-stylus strip chart recorder. The foilometer output was calibrated by firing the laser directly into a TRG model 117 Thermopile which had a factory calibrated output of 36.08 microvolt/joule. Peak laser power was calculated by dividing

the output energy by the pulse width (FWHM). This procedure is possible because the laser power as a function of time closely approximates a Gaussian distribution.

Breakdown characteristics were monitored by a capacitive voltage divider built into the RG/17 cable between the switch tank and the charging power supply (Figure 2). A schematic of this C-divider is shown in Figure 5. It was constructed by removing a 12-inch section of braided outer conductor from the RG/17 cable and replacing it with a 10-inch section of copper foil. A mylar sleeve was placed over the copper foil and a length of aluminum tubing placed over the mylar. The tubing was connected at each end to the braided copper cable shielding to complete the outer conducting path and an insulated connection was made to the copper foil. Therefore the resulting cable section had an insulated section of copper foil between the inner conductor and the outer conductor.

A signal was received from the C-divider when the tank and cable were discharged through the electrode gap. The rapidly falling field between the cable conductors induced a voltage on the copper foil which was monitored by a Tektronix 519 oscilloscope. A typical display of a C-divider signal is shown in Figure 6B. The transit time of a signal from the gap to the C-divider was calculated from coaxial formulae as 5.5 nsec. This delay from breakdown to reception by the C-divider was accounted for in delay measurements as will be discussed later.

Sample traces of the photodiode output and the C-divider output are shown in Figure 6. Trace A is the laser pulse alone; trace B is the C-divider signal alone; and trace C is for the two signals fed into

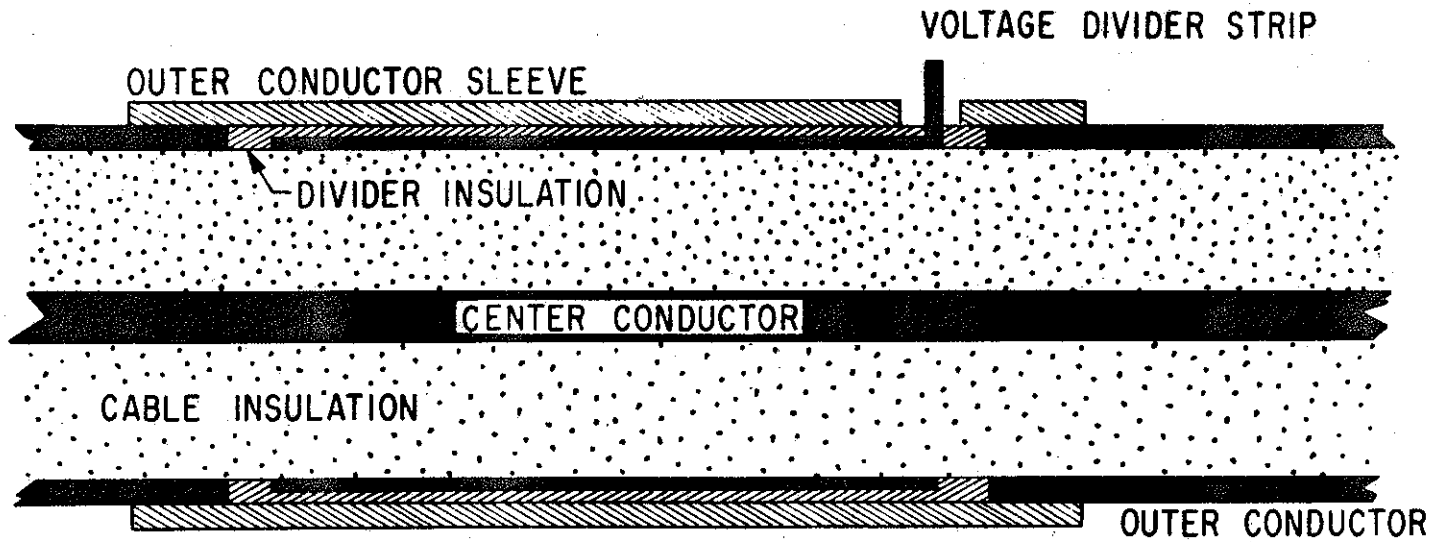

Figure 5. Schematic Detail of
Capacitive Voltage Divider

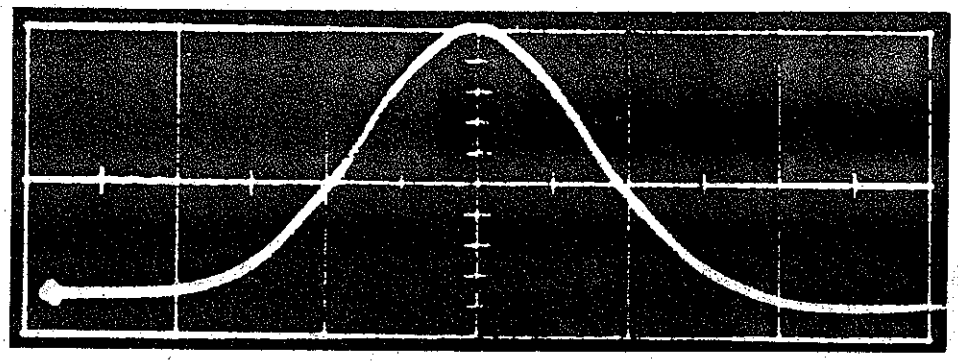

Figure 6A. Laser Pulse from Photodiode Displayed on Oscilloscope at 20 nsec/div.

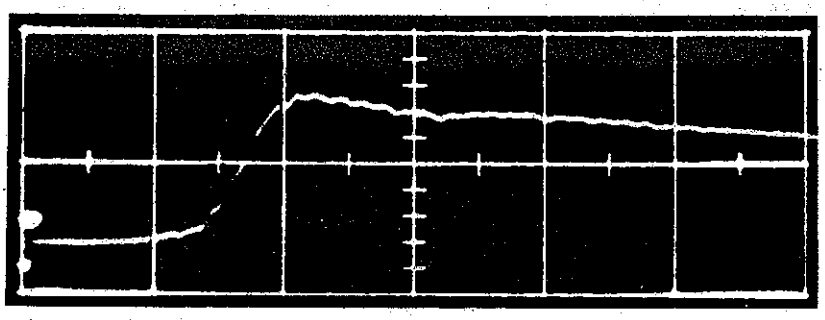

Figure 6B. Breakdown Signal from C-Divider Displayed at 5 nsec/div.

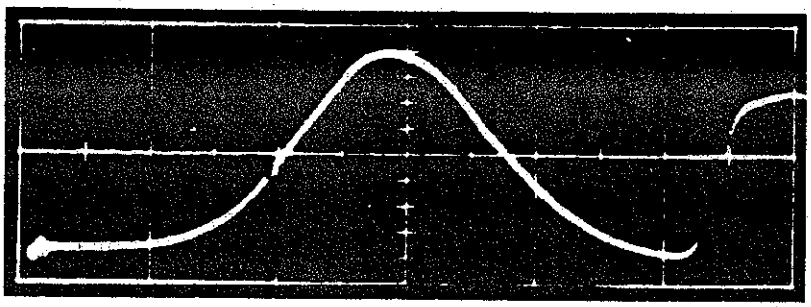

Figure 6C. Laser Pulse and Breakdown Signal on Same Trace, at 20 nsec/div.

one scope. Trace C was used to measure delay as will be explained later, and trace B was used to measure breakdown risetime (switch closure time).

Focus Determination

Focal point of the laser was determined theoretically and experimentally. The theoretical determination used simple lens equations and assumed incident parallel light. With the lens holder pushed completely into the electrode, "h" was 6.85 cm (Figure 4). The theoretical focal point versus "d" for h = 6.85 cm is shown in Figure 7. (Note: "d" is only defined with the lens holder completely in.) The experimental focal point was determined photographically. A camera was set up over the tank access port and focused on the center axis of the electrodes. The gap was opened as far as possible and h was set at 6.85 cm. Then pictures of the laser focusing in the gap were taken for successively decreasing values of d. One such picture is shown in Figure 8A.

For consistency the experimental focal point was defined as "breakdown-begin," that is, the point nearest the target electrode where the intense breakdown plume just started forming. "Breakdown-end" was defined as the point farthest from the target electrode where the intense plume ended. Thus the region from breakdown-begin to breakdown-end was the region of most intense breakdown in the oil. The points defining this region are plotted as a function of d for h = 6.85 cm in Figure 7.

The graph shows that the theoretical focal point should be about 1 mm behind breakdown-begin. This occurrence is not unreasonable because of the nature of a laser-induced plasma. That is, even though the tendency is to propagate in a direction opposite that of the laser beam (Ref. 29), a certain amount of normal expansion will occur in the

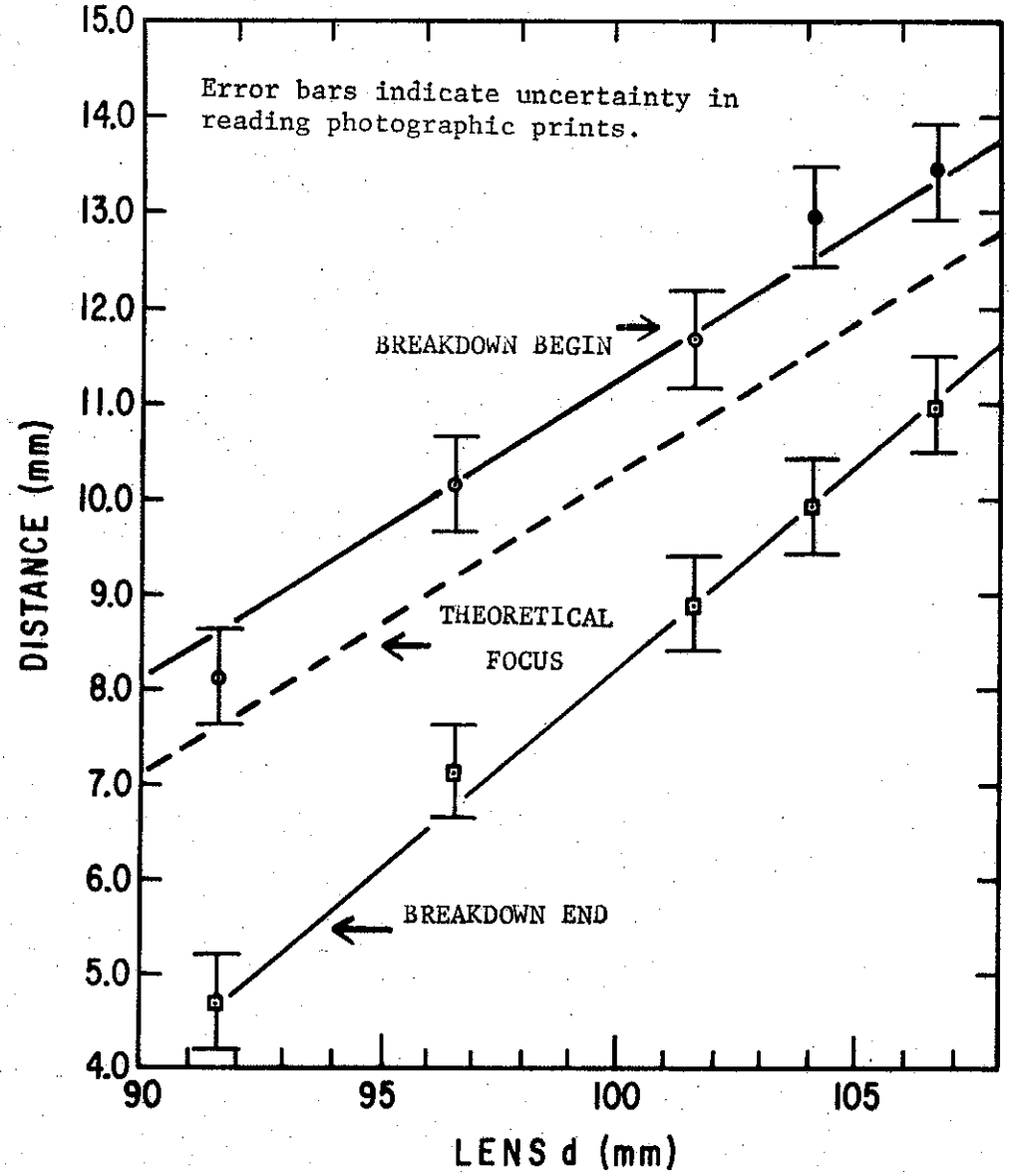

Figure 7. Laser Focusing Parameters as a Distance from Ground Electrode vs.Collecting Lens Position (d).

Figure 8A. Laser Focusing in Transformer Oil Between Switch Electrodes (1.85X).

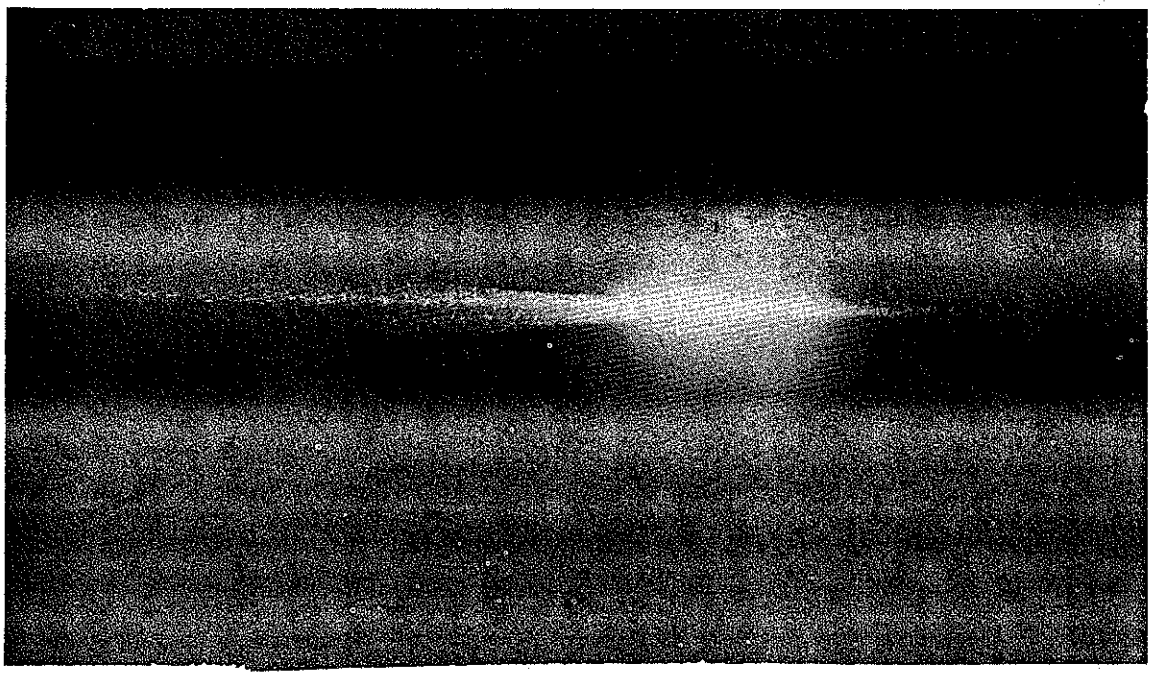

Figure 8B. Laser Focusing in Transformer Oil with 16.5 cm Lens (3.3X).

other direction. So the experimental and theoretical focal points agree reasonably well (within 10 percent).

This expansion effect is even more pronounced for longer focal length lenses because of the longer focal region obtained, as can be seen in Figure 8B. Notice that the rays seem to converge toward the center of the bright region. This picture was obtained by focusing a beam into a tank of transformer oil with a lens of focal length 16.5 cm or roughly eight times the focal length of the lens system in the electrodes.

As a matter of practical interest it might be noted that many focusing lenses were damaged in these focal point studies. This is a result of the short focal lengths of the lenses used. However, it was found that if d were set at its maximum value of 106.5 mm, one lens would last for hundreds of shots, whereas at lower values the power density going into the focusing lens was high enough to damage it after a few shots. Therefore all switching measurements were taken by setting d at 106.5 mm and pulling the entire lens holder out until the laser was focused at the desired point in the gap. The effective focal length of the double lens system in this configuration was 20 mm.

Power Density Determination

In addition to knowing where the laser focused, it was desirable to know the power density in the beam at the point where it struck the electrode. As will be shown later, the switching delay is a function of this power density, so the switching parameters are not properly defined unless focal spot size is specified in addition to peak power and pulse shape.

The first requirement for calculating spot size was to know the laser beam divergence. Using the technique described in Appendix D, the half-power beam divergence was found to be 2.5 milliradians with a shot-to-shot variation and uncertainty of 15 percent. The diameter of the half-power focal spot was obtained by multiplying this divergence by the effective focal length of the lens system.

However, as will be shown, minimum delay was achieved when the laser was focused slightly into the electrode, therefore the beam hitting the electrode was larger than the beam size at the focal point. The diameter of this slightly converging beam was calculated to be 2.08 mm with the use of equations given by Kogelnik (Ref. 23), so the half-power beam area was 3.4×10^{-2} cm^2.

Sample Preparation

Samples of the Lexan and Teflon FEP used in this research were cut from commercial grade sheets with no attempt to eliminate any pieces other than those with obvious defects such as gouges, deep scratches, or other imperfections. Sample size was chosen to be 4.5 by 5 inches to minimize the chances of dielectric breakdown around the edges of the electrodes and still allow the sample to be inserted into the tank. Before being tested, each sample was cleaned with methanol and dried with a soft paper towel.

Sample thickness was measured with a micrometer gauge over several regions of the piece and no variations were found which exceeded 10 percent of the nominal thickness. Optical absorption of the 10- to 20-mil thick dielectrics at 6943 Å was measured on a Perkin-Elmer model 350 spectrophotometer; and within the 1 percent sensitivity of the instrument no absorption was observed.

Experimental Definitions of Delay, Jitter, and Risetime

The parameters investigated in this study included laser focal point, applied voltage, electrode polarity, laser power, sample thickness, and sample type. In order to study the effects of these parameters on switching characteristics, it was first necessary to have consistent experimental definitions of the dependent variables involved: delay, jitter, and risetime.

The definition of delay used in this paper is somewhat different from that used by other researchers such as Bettis (Ref. 15) and Pendleton (Ref. 28). In their studies switching delay was defined as the time interval between points A' and B (Figure 9) minus a certain time for time-of-flight corrections. Point B is determined simply by extrapolating the rising portion of the breakdown signal back to the base line. Because of the fast rising nature of this signal it is possible to define this point as the time at which breakdown of the gap occurred. However, the laser pulse does not have such a sharp rise, and some other extrapolation is necessary. Therefore the most linear part of the laser rise was extrapolated back to the base line and the intersection of the two lines was defined as "laser-begin" (A').

This same method was not useful in this study, however, because at very high applied fields it yielded negative delays. This is physically impossible since it would require the gap to break down before the laser arrived at the gap, and it would further require only 2 nsec jitter in this breakdown. Therefore another definition was formulated which defined laser-begin as the point at which the laser signal first started to rise away from the base line, as shown in the detail in Figure 9.

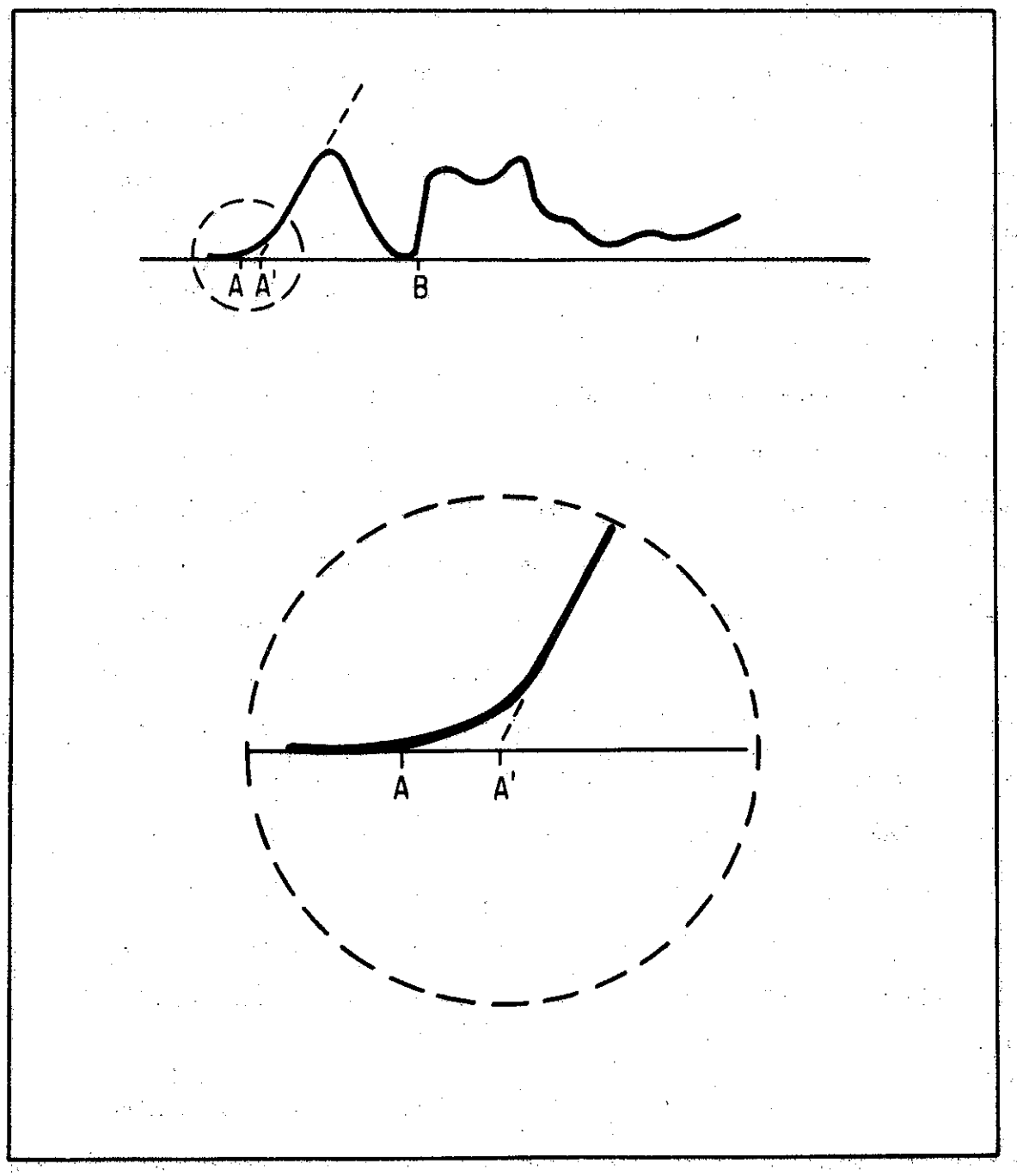

Figure 9. Diagram of Method Used to Experimentally Define Switching Delay. In this study, delay was defined as the time interval between points A ("laser-begin") and B("breakdown-begin"). At point A, as shown in the insert, the trace of the laser pulse just starts to rise away from the baseline. In previous studies (Refs. 15 and 28) "laser-begin" was defined as point A', where the linear rise of the laser pulse extrapolated back to the baseline.

When comparing the results of this study with other studies in the past or future, this difference in definitions of delay should be kept in mind because the time elapsed between points A and A' varied between 5 and 15 nsec depending upon the shape of the laser pulse. It is also believed that this method of defining delay introduces some undesirable error in measurements at very high applied fields. As will be shown later, the gap breaks down very close to the beginning of the laser pulse (point A in Figure 9) at very high fields, therefore any variation in the shape of the signal at this point will affect the measurement.

The time-of-flight correction mentioned previously deals with delays in the diagnostic system which are not inherent in the actual breakdown process. These delays include flight time from laser to gap, breakdown signal transit time to C-divider and to oscilloscope, time from laser to photodiode, diode signal to oscilloscope, and any delays added by cables in order to further separate the breakdown signal from the laser signal. The addition and subtraction of these flight times gave a constant correction time which was subtracted from the time read on the oscilloscope trace.

Jitter was defined simply as the average deviation from the mean value of delay. Risetime of breakdown (switch closure time) was defined as the time from 10 percent to 90 percent of the signal from the C-divider.

IV. RESULTS AND CONCLUSIONS

The results of this investigation are presented in this section along with a discussion of their agreement with the avalanche-streamer theory of breakdown in solids. The analysis must be at best semiqualitative, since theoretical expressions which might account for experimental results are nonexistent and empirical data on such factors in solids as ionization coefficients, recombination coefficients, and photoionization cross sections is also lacking.

Effect of Laser Focal Point Variation

Since it was desirable to optimize the ability of the laser to trigger switch closure, the first parameter studied was focal point location. The effect on switch delay and jitter of varying the focal point is shown in Figures 10 and 11. The graphs show that when the target electrode polarity was positive there was a slight but definite minimum in delay for h = 2.30 inches. For the case of a negatively charged target electrode there seems to be little difference in h = 2.25 inches and h = 2.30 inches. Values of h smaller or larger than those shown on the graphs yielded even longer delays.

On the basis of these graphs it was decided that h = 2.30 inches was the best lens setting to use for subsequent delay and jitter measurements. Although h = 2.25 inches might have been a better setting for firing into the negative electrode, it was decided that using the same focal point for both polarities would allow a better comparison of the effects introduced by polarity changes.

Using a lens setting of h = 2.30 inches resulted in the laser being focused at a point slightly into the electrode, therefore the

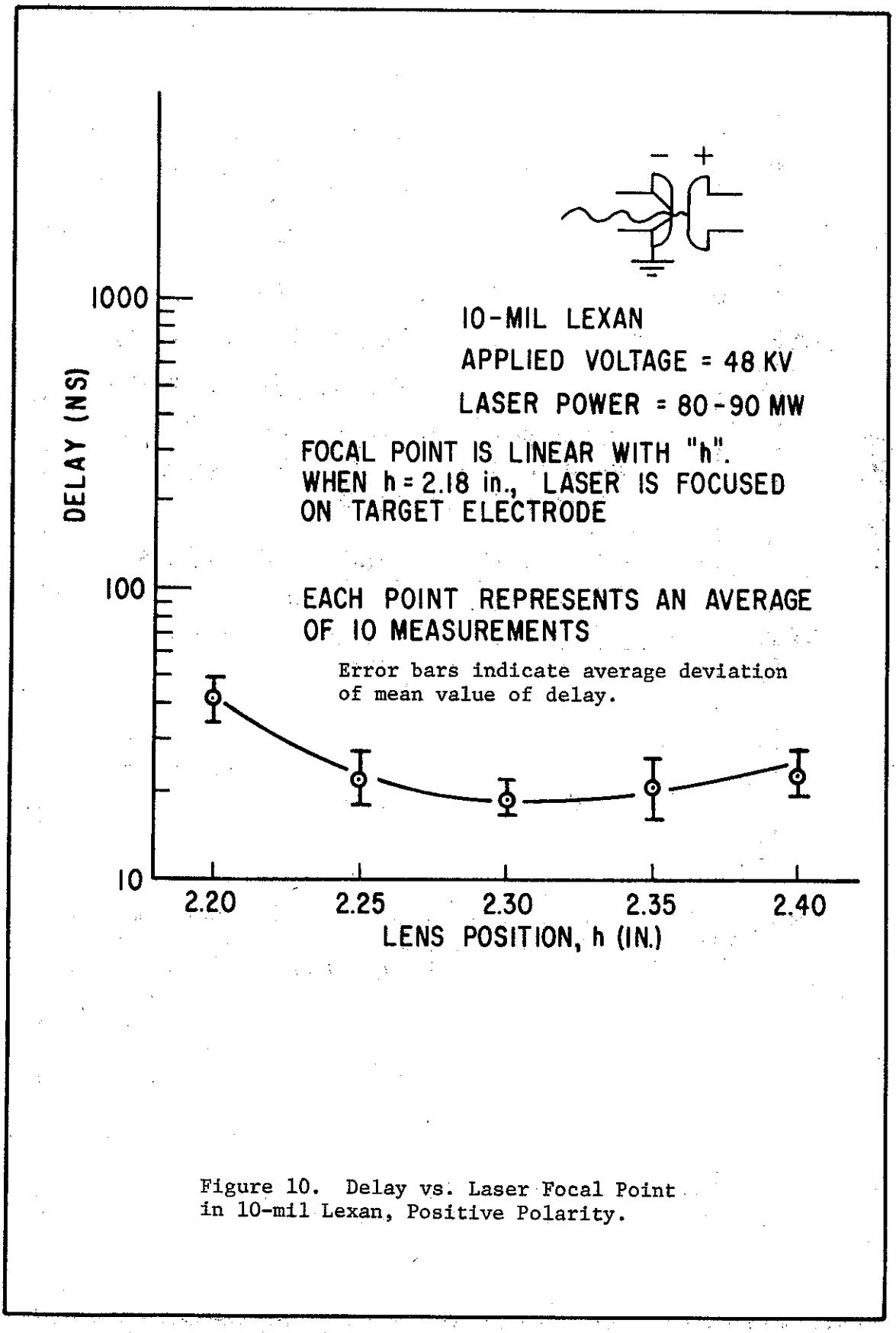

Figure 10. Delay vs. Laser Focal Point in 10-mil Lexan, Positive Polarity.

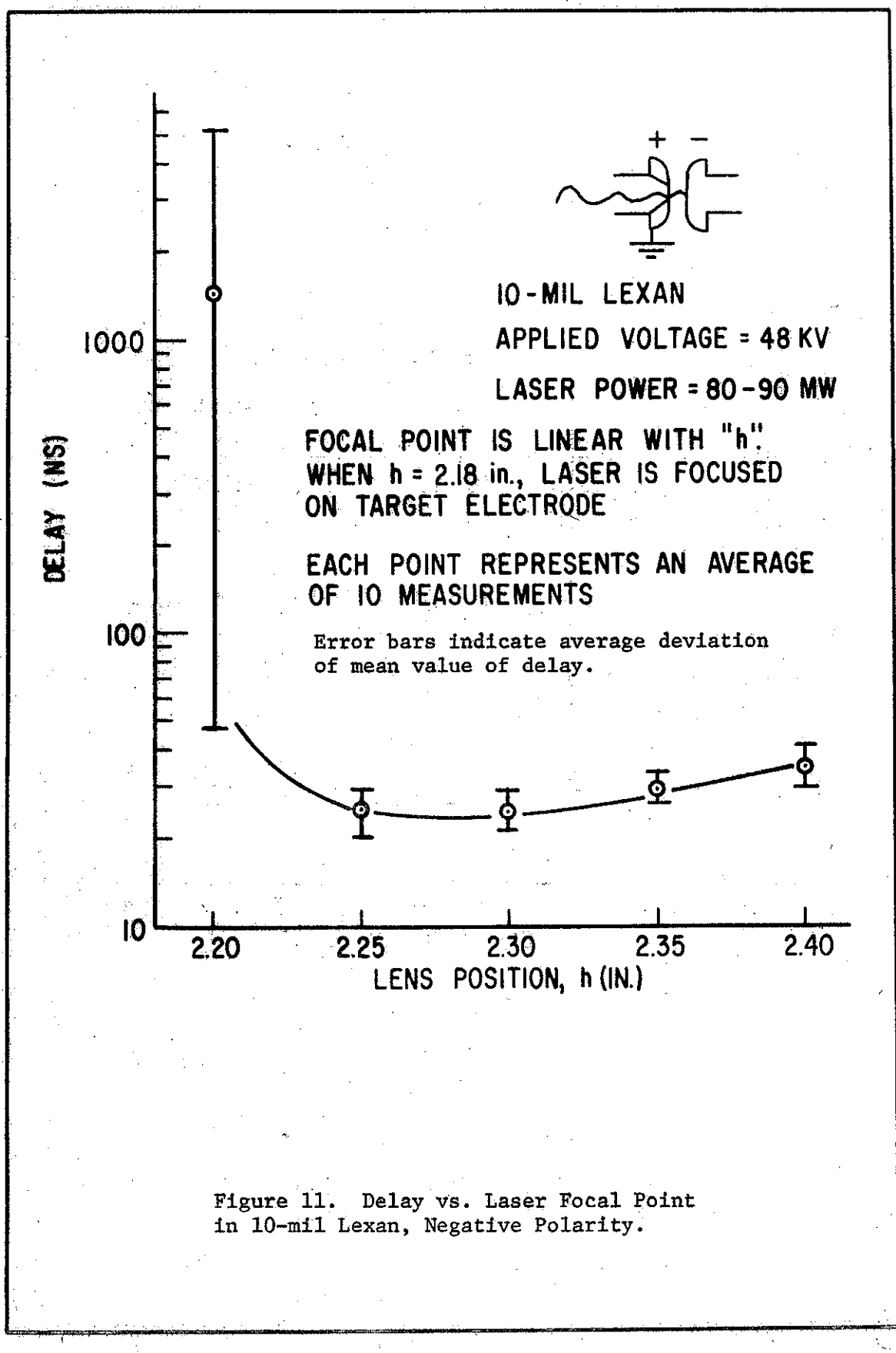

Figure 11. Delay vs. Laser Focal Point in 10-mil Lexan, Negative Polarity.

focal density was not as high as it would have been if the lens had been set to focus the laser right on the electrode surface (h = 2.18 inches). Figure 12 shows how the breakdown spot size varied with lens setting.

Effect of Applied Voltage and Polarity Variation

Figures 13 and 14 show how the voltage applied to the sample affected delay and jitter in the switching of 10-mil Lexan for both polarities and laser powers between 60 and 90 MW. There are several interesting points to notice in these graphs. The most obvious one is the sharp discontinuity which occurred at a certain value of applied voltage. The value of delay at this "transition" voltage made extreme excursions from shot to shot; however, the value plotted on the graph is an average. The actual delays measured were either in the low nanosecond region or in the low microsecond region. No values fell between the two regions.

A second point is the effect of polarity on the magnitude of delay and jitter. The jitter (indicated by error bars) was higher when the target electrode was charged positive. However, the magnitude of the delay was lower for positive polarity than for negative polarity. This effect is obvious in the high region and less well defined in the low region, but is nevertheless indicated by the fact that the delays (including jitter) extended to lower values when the charge was positive.

Effect of Laser Power Variation

Figure 15 shows the effect of reducing the peak laser power from 60 to 90 MW to 20 to 30 MW. The result was that the magnitude of delay and jitter increased, but the transition from the low delay region to the high delay region occurred at the same voltage.

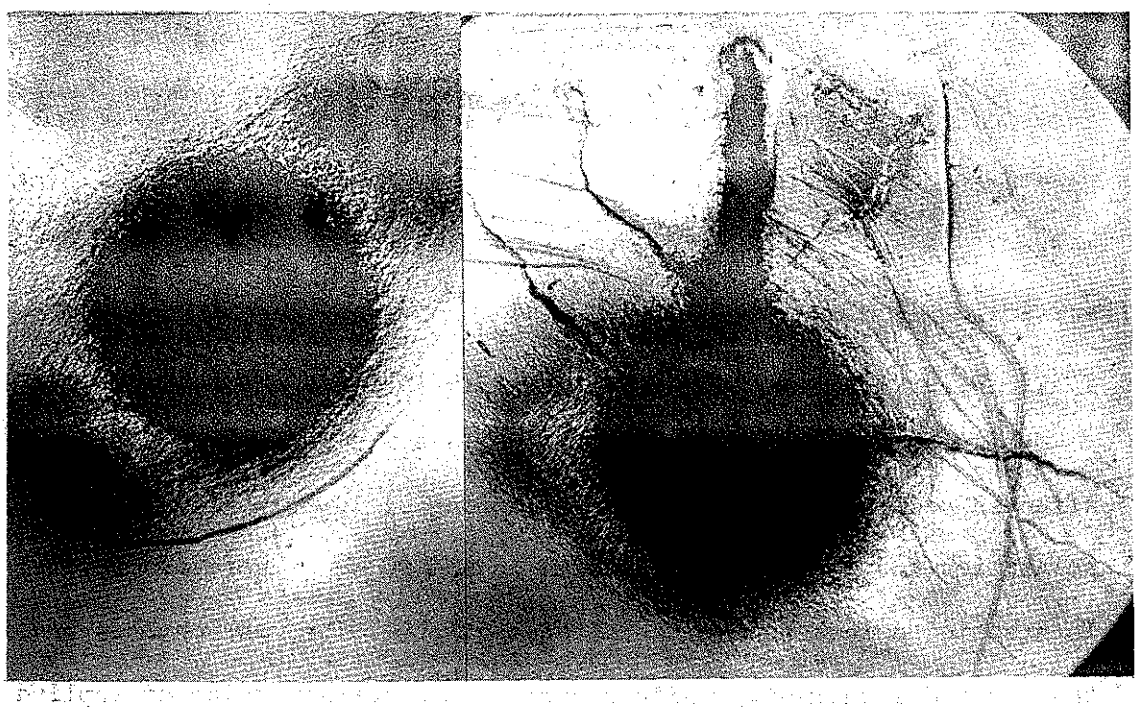

Laser Alone, h=2.3 in.

Laser and Breakdown, h=2.3 in.

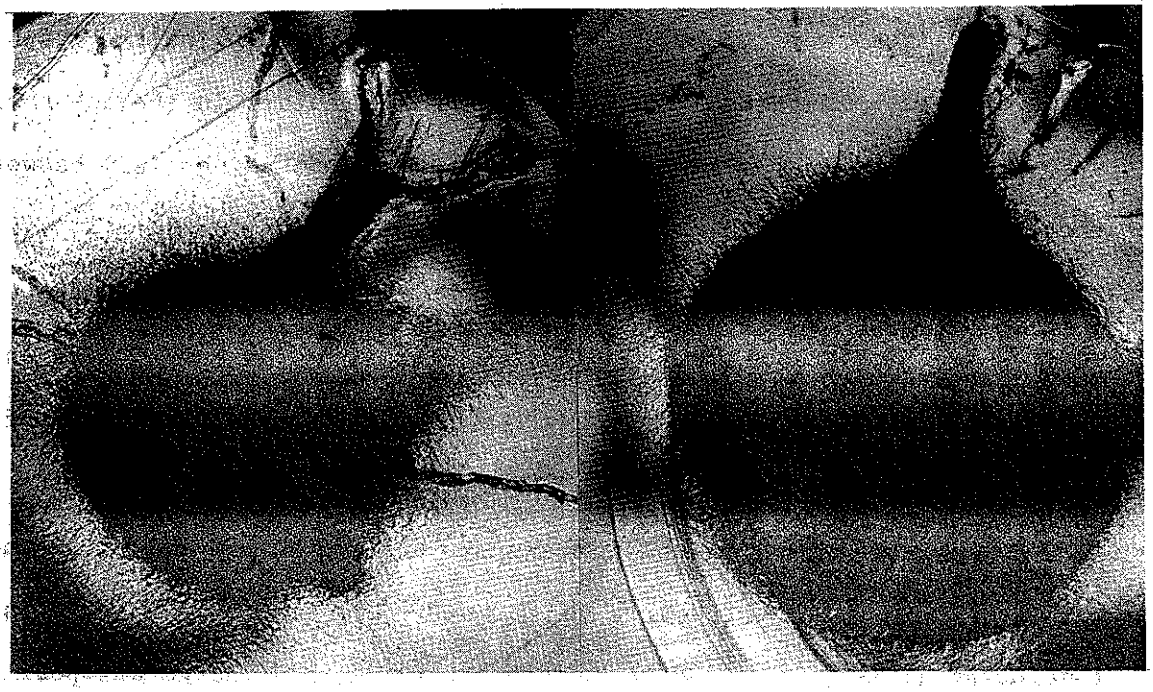

Laser and Breakdown, n=2.35 in.

Laser and Breakdown, h= 2.4 in.

Figure 12. Laser and Breakdown Damage in 10-mil Lexan (25X).

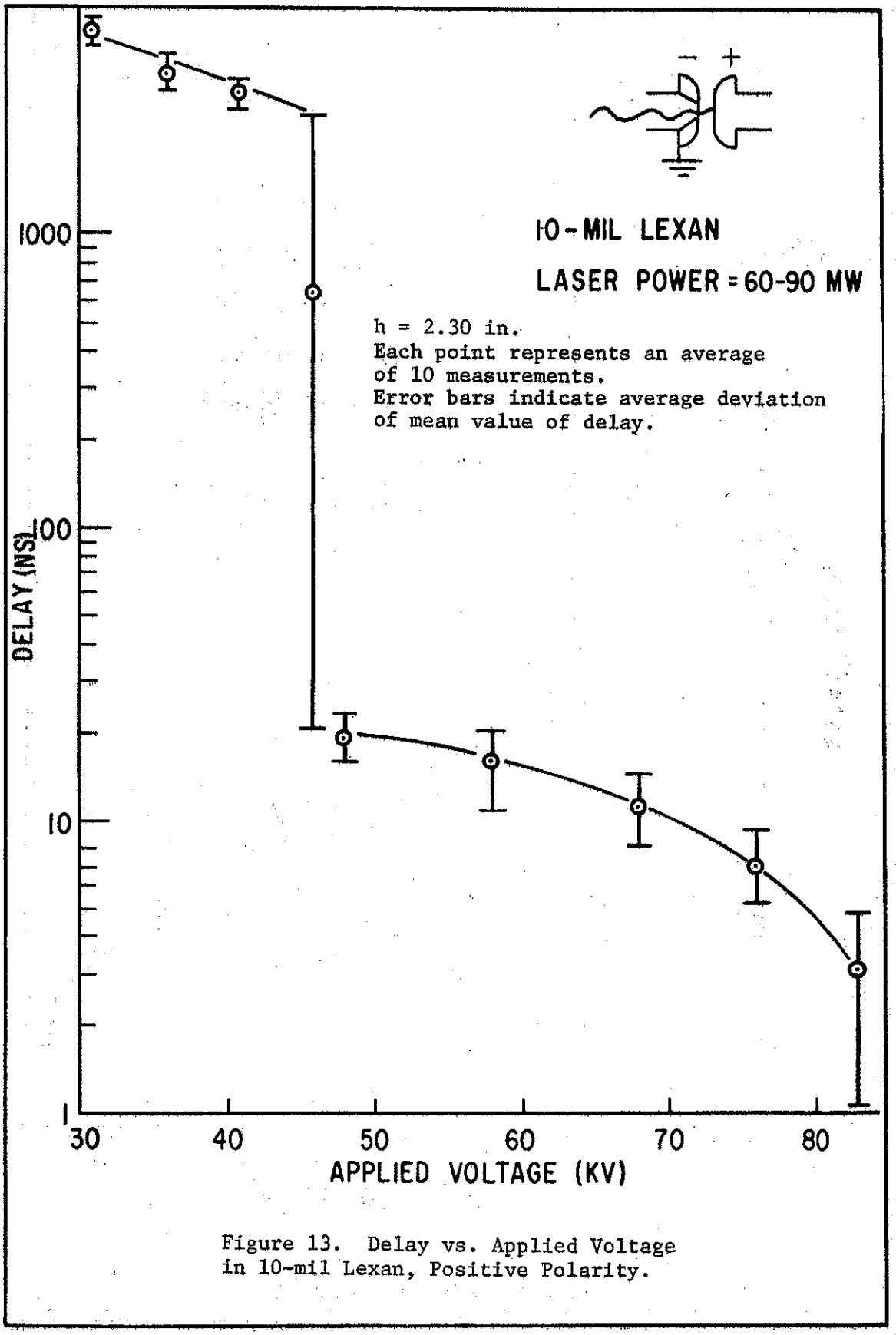

Figure 13. Delay vs. Applied Voltage in 10-mil Lexan, Positive Polarity.

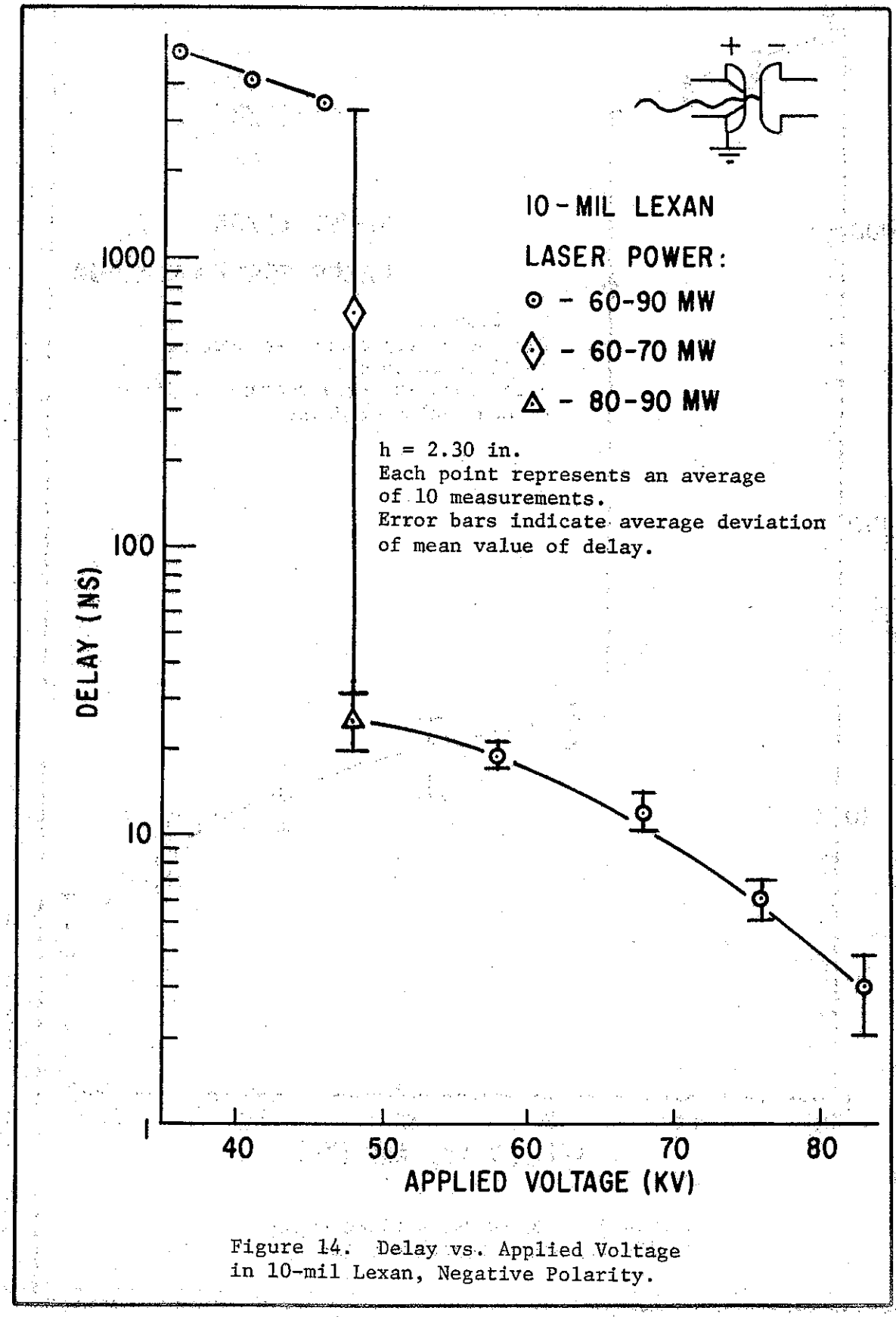

Figure 14. Delay vs. Applied Voltage in 10-mil Lexan, Negative Polarity.

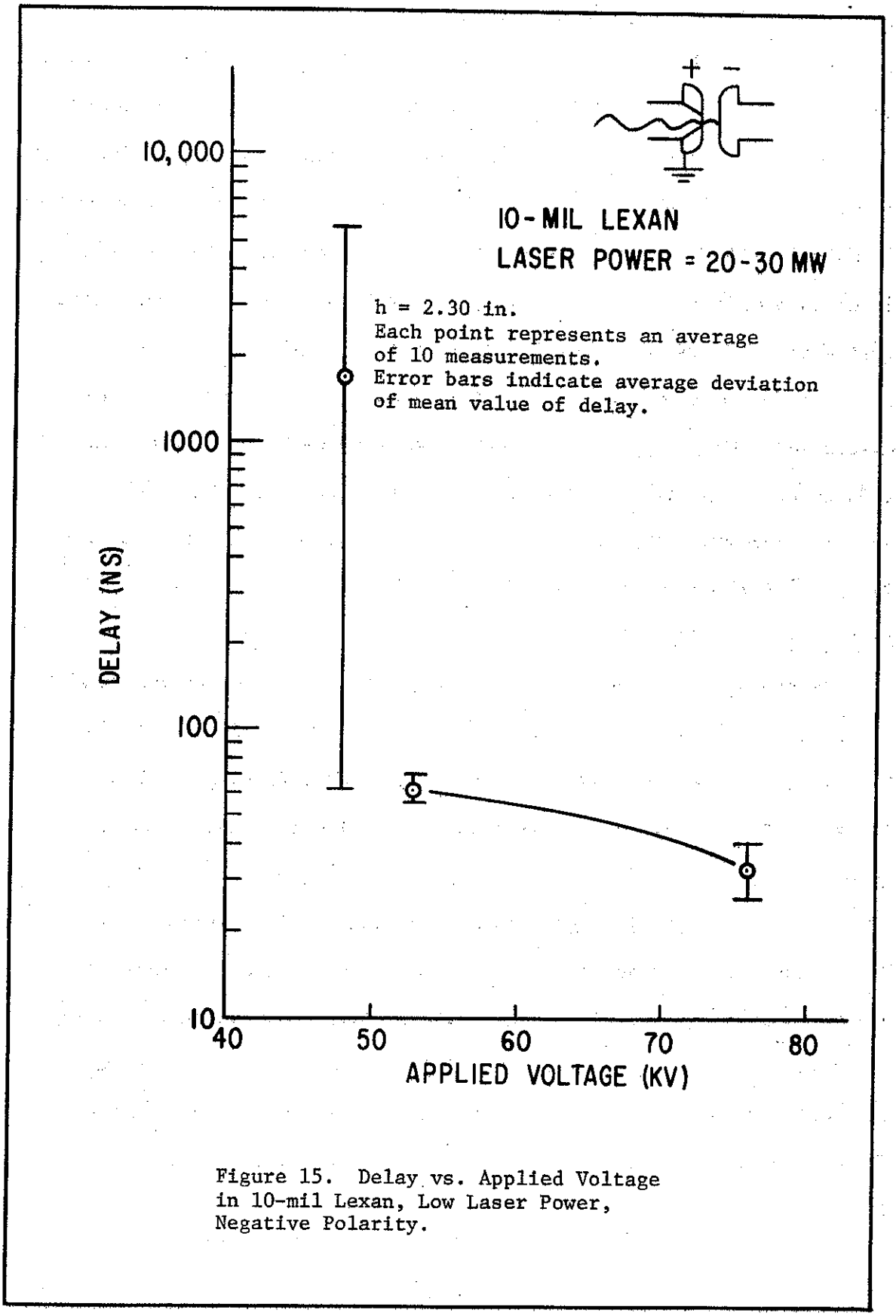

Figure 15. Delay vs. Applied Voltage in 10-mil Lexan, Low Laser Power, Negative Polarity.

Effect of Sample Thickness Variation

The effect of sample thickness on switching delay in Lexan charged to 4.1 KV/mil is shown in Figures 16 and 17. The dependence is evident; at a constant field the delay decreases with increasing sample thickness between 10 and 20 mils. Note, however, that this field is less than the transition field in 10-mil Lexan. It would have been desirable to study this effect at fields above the transition field, but the voltage limitations on the switch tank did not permit this.

It is also interesting to note that delays measured in two 10-mil sheets were about twice as high as those measured in one 20-mil sheet. This effect is probably due to one or both of the following: (1) the oil film between the 10-mil sheets, or (2) random alignment of imperfections in the two 10-mil sheets.

Effect of Material Variation

In addition to Lexan, the switching characteristics of Teflon FEP was studied. Delay versus applied voltage for 10-mil Teflon FEP is plotted in Figure 18. However, there are several factors which make it difficult to directly compare this graph with the similar one for 10-mil Lexan.

One such factor is that the self-breakdown voltage for 10-mil Teflon FEP was about 60 KV, but the 10-mil Lexan would not self-discharge even at 85 KV (the upper voltage limit for the test system). The highest published value of the dielectric strength of Lexan was 4 KV/mil, but the measurement was taken with air as the ambient medium. The oil medium used in this study increased the voltage holdoff considerably.

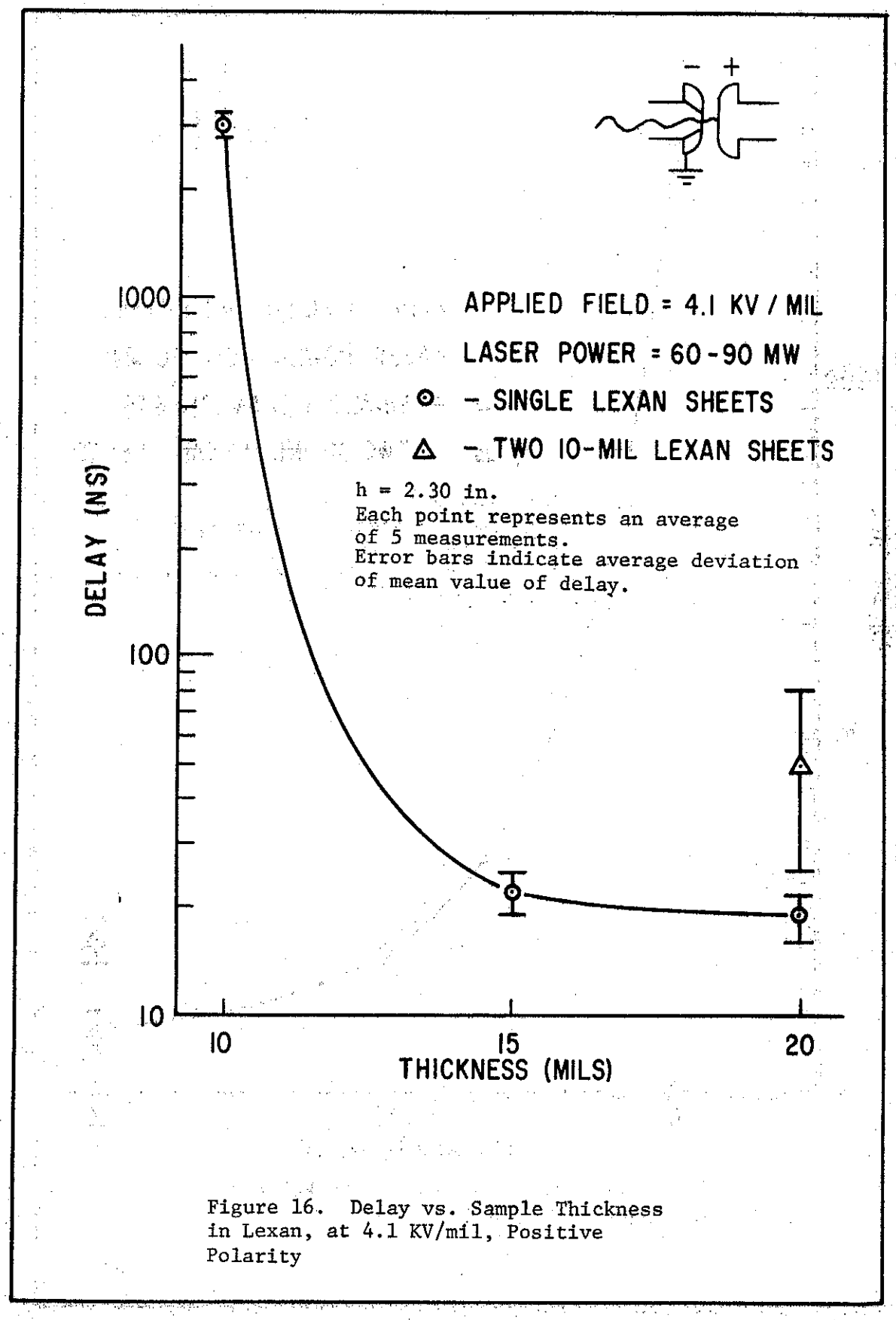

Figure 16. Delay vs. Sample Thickness in Lexan, at 4.1 KV/mil, Positive Polarity

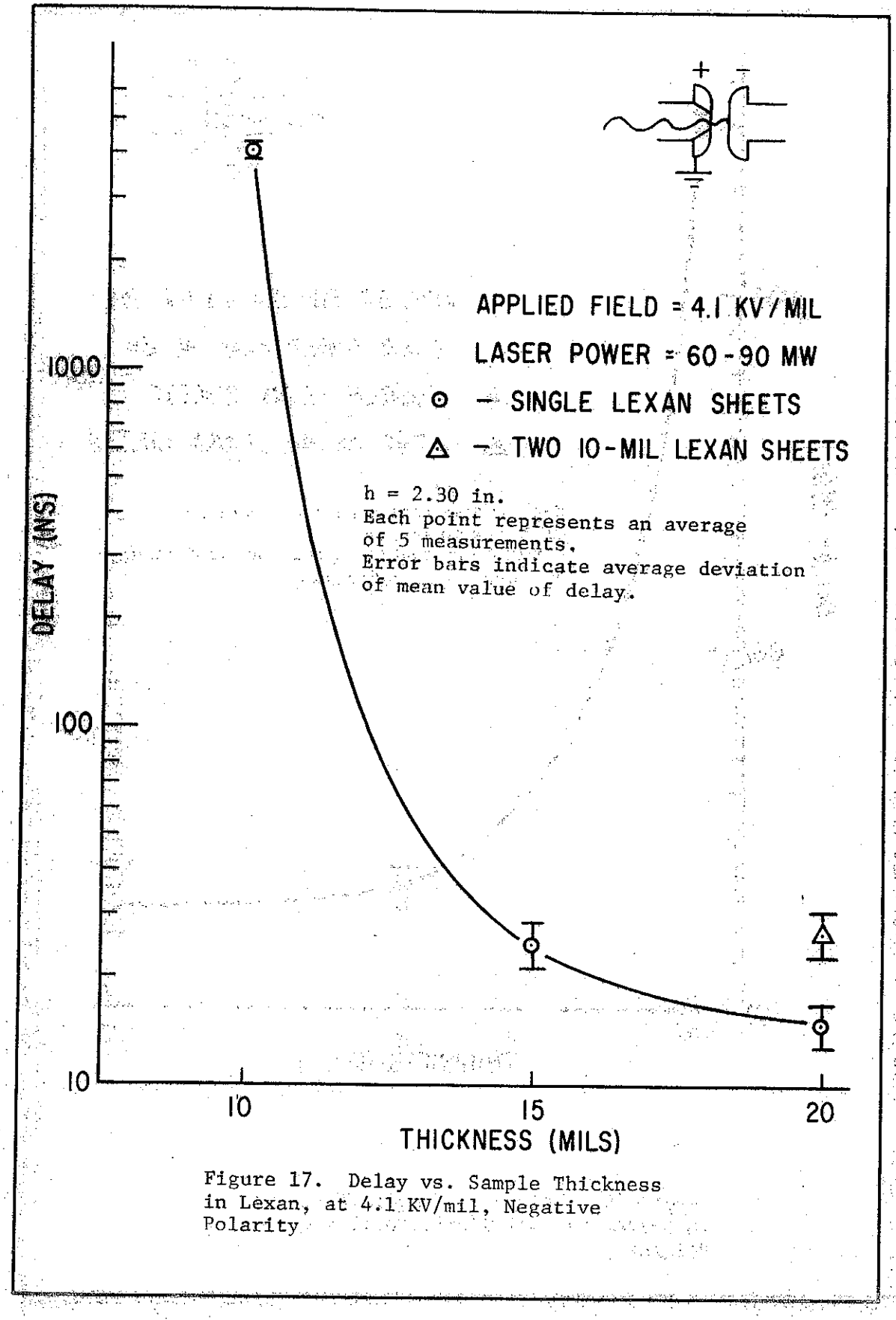

Figure 17. Delay vs. Sample Thickness in Lexan, at 4.1 KV/mil, Negative Polarity

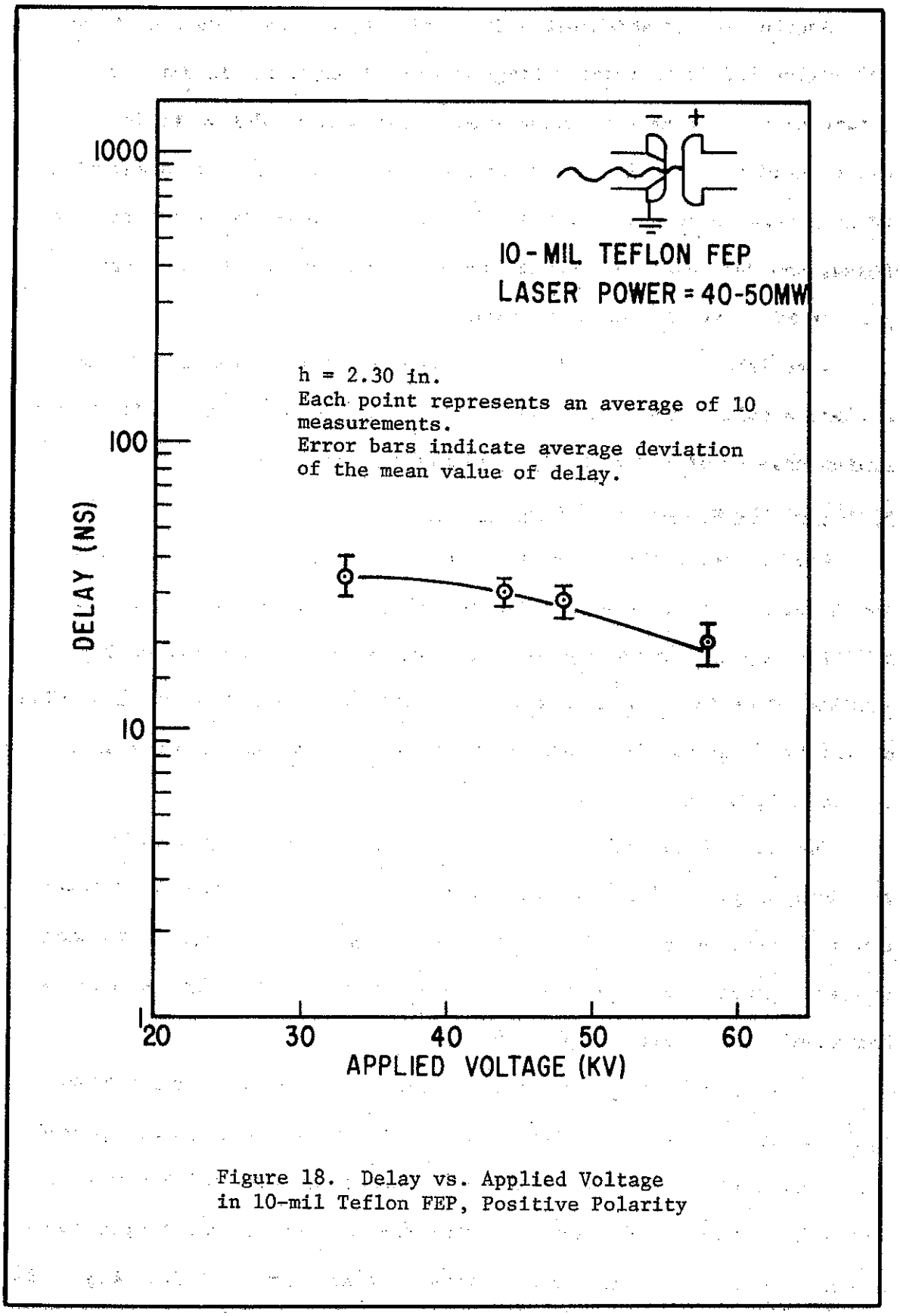

Figure 18. Delay vs. Applied Voltage in 10-mil Teflon FEP, Positive Polarity

Another factor which makes it difficult to compare data on Lexan and Teflon FEP is that the voltage was not lowered sufficiently to determine if a transition point from low nanosecond delays to low microsecond delays existed for Teflon. Nevertheless, it is interesting to note that in this solid, which has a lower dielectric strength than Lexan, nanosecond delays were achieved at voltages which would have yielded microsecond delays in Lexan.

Therefore, it might not be unreasonable to conclude that at low fields, a solid with a low dielectric strength might trigger with lower delays than a solid with a high dielectric strength.

Effect of Graded Dielectrics on Risetime

Graded dielectrics were included in this study because of their known ability to increase the voltage holdoff of a gap (Ref. 1). In addition to this advantage, Guenther believed that their use would decrease risetime (switch closure time) through the formation of multiple breakdown channels (Ref. 14). These multiple channels reduce risetime by lowering the switch impedance.

The graded dielectrics used in this study were constructed by inserting a piece of 0.5-mil aluminum foil between two sheets of 10-mil Lexan. Three types of foil inserts were used: (1) a round, 1.25-inch diameter insert, (2) a hexagonal insert with 0.6-inch sides, and (3) a hexagonal insert with 1-inch sides.

It was found that when the laser was fired into the center of the foil it caused breakdown between the center of the foil and the ground electrode, but no breakdown between the center of the foil and the target electrode. The breakdown path from the foil to the target electrode occurred at several places around the edge of the foil. Figure 19 shows a picture of this breakdown behavior.

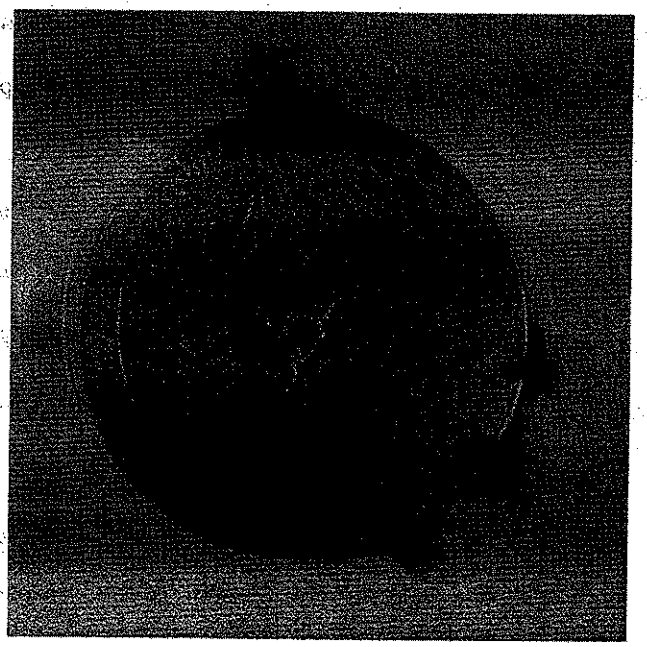

Figure 19. Multi-Channel Breakdown Behavior of Graded Dielectric. 1 in. Diameter, Round Insert

These dielectrics broke down around the edges of the foil because of strong field enhancement there. The number of channels that occurred could not be controlled, but was probably dependent upon the number and physical nature of the field-enhancing defects that were produced around the edge of the foil in the process of cutting.

Figure 20 shows how the number of these breakdown channels affected switch risetime. The expected effect would be that the risetime would decrease with increasing channels but as can be seen this occurs only for the round insert and for the small hexagonal insert. The opposite effect occurs for the large hexagonal insert and no explanation for this apparent inconsistency can be proposed at this time. However, it is possible to draw the general conclusion that the use of graded dielectrics provides means of using a single laser beam to initiate multiple breakdown channels in solids with a subsequent reduction in switch risetime.

No correlation could be found between delay and risetime in these dielectrics. Delays in all of them were about the same as the delay in 20-mil Lexan.

Summary

In order to better analyze the main results of this study, they are first summarized for convenience.

1. Minimum delay was achieved when the laser was focused 0.12 inches inside the target electrode.

2. Delay in Lexan increased continuously as applied voltage decreased until a transition voltage was reached where the delay increased discontinuously with extremely high jitter. Below the transition voltage the delay again increased continuously with decreasing voltage but at

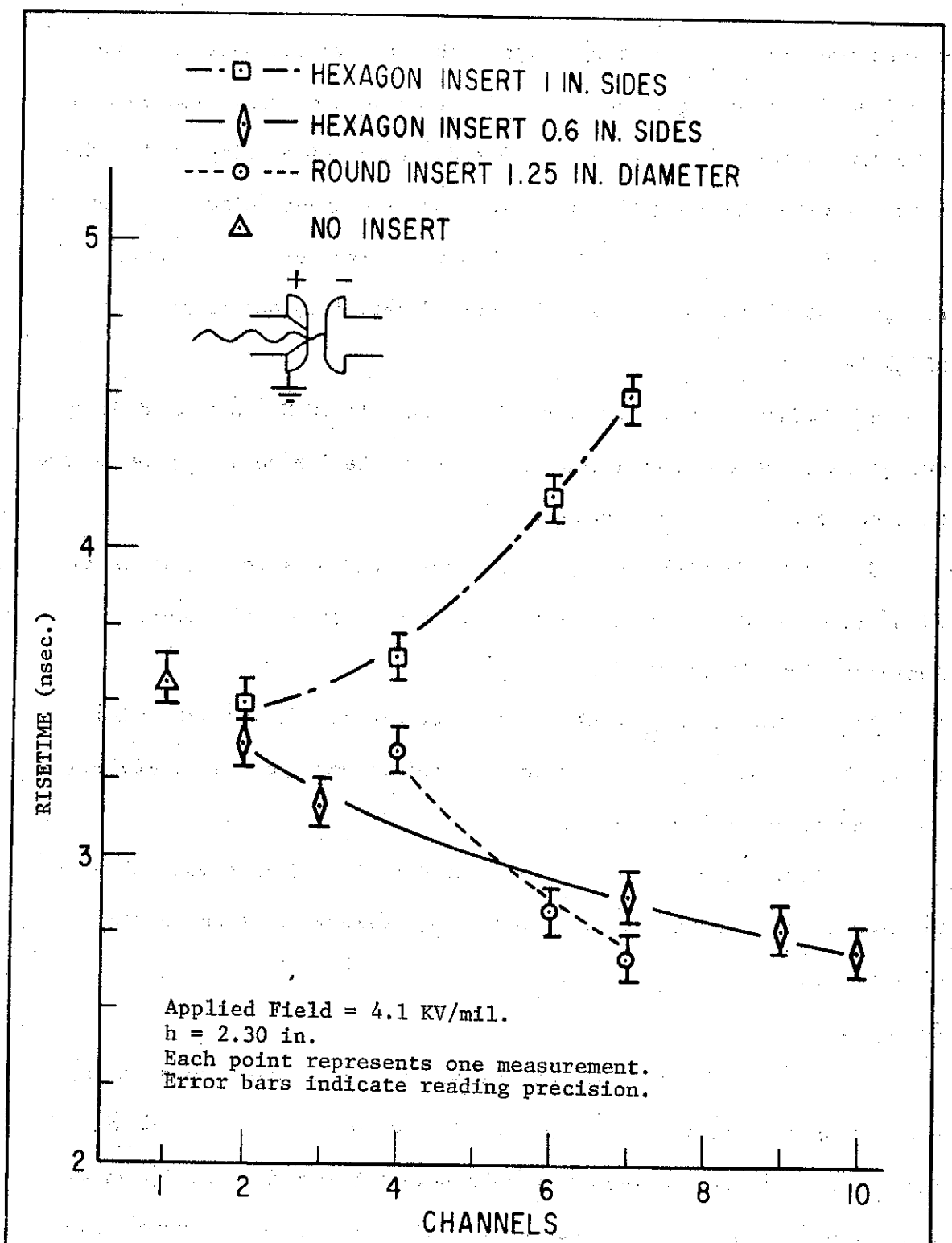

Figure 20. Variation of Risetime With Number of Breakdown Channels In Graded Dielectric

values two orders of magnitude higher than the values measured above the transition voltage. Values of delay above the transition voltage were always less than the laser pulse duration while delays below the transition voltage were always longer than the laser pulse duration.

3. Delay was somewhat lower when the target electrode was charged positive than when it was charged negative, but jitter was slightly higher.

4. Reduction of laser power from 90 MW to 20 MW increased delay and jitter, but the transition voltage from the low delay region to the high delay region did not change.

5. At an applied field of 4.1 KV/mil (which is below the transition field in 10-mil Lexan) delay decreased as sample thickness increased from 10 to 20 mils.

6. In Teflon FEP, which has a lower dielectric strength than Lexan, low nanosecond delays were achieved at voltages which yielded low microsecond delays in Lexan.

7. It was possible with one laser beam to initiate multiple breakdown channels in graded dielectrics, thereby reducing switch closure time.

Discussion

It is believed that the results of this study are consistent with the avalanche-streamer theory of solid breakdown. This conclusion is first indicated by the fact that delays were lower when breakdown was initiated from the anode. Second, equation (9) allows a semiqualitative explanation of how the other parameters affected delay.

$$t_d \approx \frac{1}{2\sqrt{\gamma(A_1+A_1)}} \ln \left[\frac{\sqrt{\frac{A_1+A_2}{\gamma N_\Sigma^2}} + 1}{\sqrt{\frac{A_1+A_2}{\gamma N_\Sigma^2}} - 1} \right] \qquad (9)$$

It has already been shown how this equation relates to triggered breakdown of an under-volted solid. It also indicates that t_d should increase as the applied voltage decreases. This effect is primarily due to the decrease in α with applied field. As α decreases, A_2 decreases exponentially and t_d increases.

It might, at first glance, be expected that this trend should continue smoothly until the gap no longer breaks down, even with the aid of the laser (i.e., A_2 decreases until $A_1 + A_2 = \gamma N_\Sigma^2$). However, to show that this trend is discontinuous rather than continuous, let us postulate that at a certain applied voltage, V_t, the gap has not broken down after a time t_ℓ (length of laser pulse). At this point the laser production term A_1 will be removed from equation (9) because the laser pulse has ended. In addition, because of the rapid expansion velocities of the laser-induced plasma, a great deal of the charge accumulated during t_ℓ will be eliminated.

The resulting effect is that in a time probably no greater than about 5 nsec, the laser stops aiding in the space charge buildup, and most of what charge had accumulated up to that point is dissipated through both expansion and recombination. We now have a completely different situation than we had before the laser was fired. Before t_0, $A_2 = \gamma N_\Sigma^2$ so that $t_d = \infty$. Now, however, because of the damage done to the dielectric by the laser, the values of A_2 and γ have changed. A_2

has increased to A_2' because α' in the damaged dielectric is greater than α in the virgin dielectric, and γ has decreased to γ'. The new condition is $A_2' > \gamma' N_\Sigma^2$ so that the material is slightly over-volted. The gap then proceeds to break down at a rate which depends upon A_2' and γ'. The resultant breakdown times are expected to be considerably greater than those obtained when the laser term A_1 assists breakdown.

Thus the delay is split into two regions:

(1) $t_d \leq t_\ell$ (low region) where breakdown is determined by A_1, A_2, and γ, and

(2) $t_d >> t_\ell$ (high region) where breakdown is determined by $A_1 = 0$, $A_2' > A_2$, and $\gamma' < \gamma$.

This postulated mechanism agrees with experimental data. That is, when $t_d \leq t_L$, breakdown is in nanoseconds. However, if $t_d > t_L$, it is greater by two orders of magnitude. This same effect, while not so extreme, was also observed by Bettis in gases (Ref. 3), Marolda in DC-charged transformer oil (Ref. 25), and Zigler in pulse-charged transformer oil (Ref. 39).

The increase in delay with a reduction in laser power is to be expected. This effect results simply from a decrease in the magnitude of A_1. However, it also might be expected that further reduction of laser power would increase the transition voltage (V_t) in addition to increasing delay.

The decrease in delay with increasing thickness is also reasonable in light of equation (9). The factor here which reduces t_d is the dependence of A_2 on d (sample thickness), since $A_2 \propto 2^{\alpha d}$. However, two qualifications must be made concerning this observation. First, the applied field was just below the transition field, so that a slight

increase in A_2 was enough to drop t_d back into the time regime of the laser pulse. For fields above the transition field, this thickness effect would probably not be so marked. The second qualification is that no conclusion can be made about how t_d will behave as thickness is increased above 20 mils. Certainly one would expect to reach a point where delay began to increase as thickness increased, because of less laser-induced damage to the dielectric.

Finally, the observed effect of dielectric strength on t_d is reasonable. A comparison of Figure 13 with Figure 18 shows that the weaker dielectric (Teflon) yields nanosecond delays at lower fields than does the stronger dielectric (Lexan). The Teflon has a higher α (higher A_2) than does the Lexan so there is greater avalanche enhancement of space charge buildup. The resulting effect is a lowering of V_t. Figures 13 and 18 cannot be compared directly, however, because the Teflon data was obtained at a lower laser power.

Recommendations

It is obvious that much more work is needed in solid dielectric laser-triggered switching before its full value can be assessed. One important study needed is the switching of thick samples DC-charged and pulse-charged to megavolt potentials. Also, more information is needed on many different materials at extreme ranges of laser powers in order to determine the best material to use and the minimum laser power needed to perform a particular switching task.

Another area which would yield valuable information about the nature of laser switching of solid dielectrics would be a study of how the transition voltage in a particular sample varied with laser pulse length. It is believed that longer pulse lengths (>100 nsec) would

yield nanosecond switching delays at lower voltages than can be obtained with relatively short pulses (<50 nsec).

Bibliography

1. Alston, L. L., High Voltage Technology. Oxford University Press (1968).

2. Barbini, S., "Arc Triggering by Means of a Laser and Technology of the Connected Spark Gap," 4th Symposium on Engineering Problems in Thermonuclear Research, Frascatti, Italy (1966).

3. Bettis, J. R., Private Communication.

4. Bettis, J. R., and Guenther, A. H., "Low-Jitter, High-Repetition Rate, Laser-Triggered Switching," to be published in IEEE Journal of Quantum Electronics.

5. Bruce, C. W., and Collet, E., Laser Instrumentation. AFWL-TR-64-127, AD 364551, Air Force Weapons Laboratory, Kirtland AFB, New Mexico (June 1965).

6. Bruce, F. M., "Calibrated Uniform-Field Spark Gaps for High Voltage Measurements at Power Frequencies," Journal of the Institution of Electrical Engineers (GB), 94: 138-49 (April 1947).

7. Clark, R. J., Laser-Triggered Switch Study. RADC-TR-68-355, Rome Air Development Center, Griffiss AFB, New York (December 1968).

8. David, C., et al., "Density and Temperature of a Laser-Induced Plasma," IEEE Journal of Quantum Electronics, QE-2: 493-9 (September 1966).

9. Dawson, J. M., "On the Production of Plasmas by Giant-Pulse Lasers," The Physics of Fluids, 7: 981-7 (July 1964).

10. Deutsch, F., "Triggering of a Pressurized Spark Gap by a Laser Beam," British Journal of Applied Physics, 1: 1711-9 (1968).

11. Ehler, A. W., "Plasma Formed by a Laser Pulse on a Tungsten Target," Journal of Applied Physics, 37: 4962-6 (December 1966).

12. Gilmour, A. S., and Clark, R. J., Laser-Triggered Switch Study. RADC-TR-67-45, Rome Air Development Center, Griffiss AFB, New York (February 1967).

13. Guenther, A. H., "Recent Developments in LTS," DASIAC Special Report 80, Defense Atomic Support Agency, Washington, DC, 2155 (September 1968).

14. Guenther, A. H., Private Communication.

15. Guenther, A. H., and Bettis, J. R., "Laser-Triggered Megavolt Switching," IEEE Journal of Quantum Electronics, QE-3: 581-8 (November 1967).

16. Guenther, A. H., and Bettis, J. R., "Nanosecond-Synchronization, Multigap-Laser-Triggered Switching," to be published in the IEEE Journal of Quantum Electronics.

17. Guenther, A. H., and McKnight, R. H., "A Laser-Triggered 50 pps High-Voltage Switch with Nanosecond Jitter," Proceedings of the IEEE, 55: 1504 (August 1967).

18. Honig, R. E., "Laser-Induced Emission of Electrons and Positive Ions from Metals and Semiconductors," Applied Physics Letters, 3: 8-11 (July 1963).

19. Honig, R. E., and Woolsten, J. R., "Laser-Induced Emission of Electrons, Ions, and Neutral Atoms from Solid Surfaces," Applied Physics Letters, 2: 138-9 (April 1963).

20. Iannuzzi, M., and Williamson, R., "Effects of Absorption of Laser Radiation on Metals," Il Nuovo Cemento, 36: 2410-14 (16 April 1965).

21. Kawamura, H., and Masami, O., "Statistical Time Lag and Electron Avalanche in Dielectric Breakdown of Mica," Journal of the Physical Society, Japan, 8: 6731-3 (November-December 1953).

22. Kawamura, H., et al., "The Statistical Time Lag of the Dielectric Breakdown of Mica, Glass, and KCl," Journal of the Physical Society of Japan, 9: 4541-5 (July-August 1954).

23. Kogelnik, H., "Imaging of Optical Modes--Resonators with Internal Lenses," Bell System Technical Journal, 455-94 (March 1965).

24. Loeb, Leonard B., Spark Breakdown in Uniform Fields. Office of Naval Research, Technical Report, Washington, DC (July 1954).

25. Marolda, A. J., "Laser-Triggered Switching in a Liquid Dielectric," IEEE Journal of Quantum Electronics, 503-5 (August 1968).

26. Meyerand, R. G., and Haught, A. F., "Optical-Energy Absorption and High Density Plasma Production," Physical Review Letters, 13: 7-9 (July 1964).

27. O'Dwyer, J. J., "The Theory of Avalanche Breakdown in Solid Dielectrics," Journal of Physics and Chemistry Solids, 28: 1137-44.

28. Pendleton, W. K., and Guenther, A. H., "Investigation of a Laser-Triggered Spark Gap," Review of Scientific Instruments, 36: 1546-50 (November 1965).

29. Raizer, Yu P., "Breakdown and Heating of Gases under Influence of a Laser Beam," Soviet Physics Uspekhi, 8: 650-73 (March-April 1966).

30. Ready, J. F., "Mechanism of Electron Emission Produced by Giant Pulse Laser," Physical Review, 37: A620-3 (18 January 1965).

31. Skeen, C. H., and York, C. M., "Laser-Induced 'Blow-Off' Phenomena," Applied Physics Letters, 12: 369-71 (June 1968).

32. Stratton, R., "The Theory of Dielectric Breakdown in Solids," Progress in Dielectrics, 3: 235-91, John Wiley & Sons, Inc., New York (1961).

33. Vorobev, A. A., and Vorobev, G. A., "Certain Rules of Electrical Breakdown of Solid Dielectrics." FTD-MT-24-193-67, AD-66 9431, USAF Systems Command-FTD (6 October 1967).

34. Vorobev, A. A., et al., "Propagation of Discharge in Single Crystals of NACL and KCL," Soviet Physics, Solid State, 2: 1814-8.

35. Vorobev, A. A., et al., "Process of Discharge Formation in Solid Dielectrics," Soviet Physics, Solid State, 3: 2376-9 (May 1962).

36. Watson, D. B., et al., "Some Aspects of Dielectric Breakdown of Solids," IEEE Transactrons on Electrical Insulation, EI-1: 30-7 (November 1965).

37. Winer, I. M., "A Self-Calibrating Technique for Measuring Laser Beam Intensity Distribution," Applied Optics, 5: 1437-9 (September 1966).

38. Yura, H. T., "The Interaction of Laser Light with Metals," Memorandum RM-3560-PR, RAND Corporation, Santa Monica, California (March 1963).

39. Zigler, G., "LTS of Pulse-Charged Liquids," to be submitted as Thesis for M.S. degree, USAF Institute of Technology, Wright-Patterson AFB, Ohio.

APPENDIX A

BRUCE ELECTRODES

Since this study involved a determination of factors affecting switch performance, it was desirable to minimize external influences such as asymmetric fields. Bruce electrodes (Ref. 6) were chosen because they meet this uniform field requirement and because they are readily machinable.

The contour of this type of electrode is shown in Figure 21. It consists of three parts, each merging tangentially into the next: (a) a flat surface AB of diameter not less than the maximum spacing at which the electrodes are to be used, (b) a portion BC of gradually increasing curvature to minimize edge effects, the initial radius of curvature being not less than 10 times the maximum gap spacing, and (c) a circular portion CD to complete the edge.

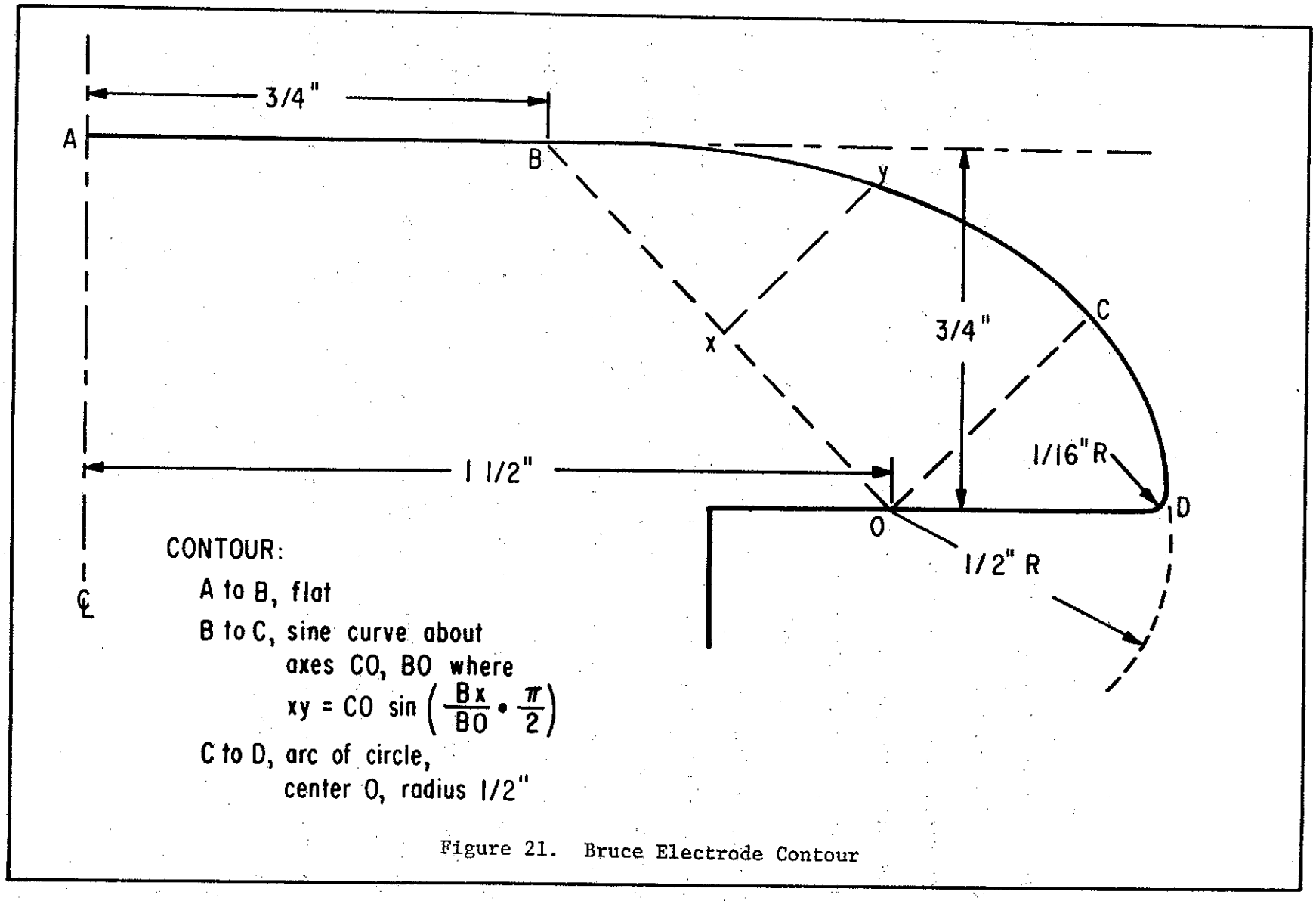

Figure 21. Bruce Electrode Contour

APPENDIX B

BLEACHABLE DYE (PASSIVE) Q-SWITCH

Q-switching is a method which is generally used to attain the highest possible peak power output of a laser. It consists of decreasing the optical gain in the laser cavity while the active medium is being inverted. Then when the medium has been excited to its maximum population inversion, the gain is suddenly increased allowing the stored energy to be released in a short burst of light.

The passive, bleachable dye Q-switch was chosen for this study because of its simplicity and economy. Also, we had no need to precisely control when the giant pulse occurred. Because of this inability to command fire a passive Q-switch, it would not be suitable for use in a critically-timed laser-triggered switching system.

A passive Q-switch operates on the principle of nonlinear absorption. Its optical transmission at the laser frequency is a function of the intensity and duration of exposure to the laser. When placed between the laser crystal and an end reflector, it acts as a nonlinear gain control switch. As rod pumping begins, the initial transmission is very low and the dye attenuates light directed toward it. Then when the rod has been pumped sufficiently hard, a rapid absorption occurs in the dye which bleaches it out and creates a condition of high gain. This sudden gain increase rapidly depletes the inverted medium and a giant pulse of light is emitted. The power output is determined by the dye concentration and and the amount of optical pumping.

APPENDIX C

OSCILLOSCOPE CALIBRATION

Because of the extremely short times involved in LTS, it was necessary to ensure that the scopes used to measure these times were accurately calibrated. The Tektronix 519 oscilloscopes were calibrated on the 5, 10, 20, and 50 nsec/cm sweep speeds by the injection of a 250-MHz signal from a General Radio type 1215C oscillator. Accurate measurement of the injected signal frequency was made with a Hewlett-Packard type 5257A transfer oscillator in conjunction with a Hewlett-Packard type 5245L frequency counter. This combination gave better than five-figure accuracy in frequency monitoring.

The signal thus displayed on the scope at the various sweep speeds was photographed and read on a Carl Zeiss model 1047 film reader. The accuracy of the film reader was limited by operator error to about $\pm$0.05 mm of film distance or $\pm$0.1 mm of actual distance (camera reduced image by a factor of 2). Therefore, at 20 nsec/cm the uncertainty in sweep speed was 0.2 nsec/cm.

The resulting correlation between real time and distance on the film gave the sweep calibration for that scope and sweep speed. It was found that in all cases the initial part of the trace showed nonlinearity up to a certain point beyond which the trace was linear. This nonlinear portion was, for most scopes, no more than the first half centimeter of trace. It was corrected for by externally triggering the oscilloscopes and delaying the input signal until the trace had passed

the nonlinear part. Therefore all measurements of laser and breakdown characteristics were made in the linear region of the oscilloscope trace.

APPENDIX D

BEAM DIVERGENCE MEASUREMENT

Beam divergence was measured using a technique described by Winer (Ref. 37). The technique yields quantitative photographic determinations of laser intensity distributions. The self-calibrating nature of the method eliminates the effects of nonlinear response among different photographic emulsions.

It involves focusing the laser beam on a smooth MgO block with a long focal length lens ($\sim$3 meters). The focused image is then photographed through a multiple lens plate which gives many images on one photographic plate. Behind the lenses are placed filters of various calibrated neutral densities and the resulting multiple images have different densities.

Upon being scanned with a densitometer, these images yield the intensity distribution across the laser beam. This information is then reduced by the method described in reference 37 and yields a plot of relative energy density versus full cone divergence angle. Beam divergence is then defined as the full cone angle at which the relative energy density falls to 1/2 its maximum value (1/2 power beam divergence). The uncertainty in the quoted value of beam fivergence is the maximum and minimum deviation in fitting a curve to the experimental data, as illustrated in Figure 22.

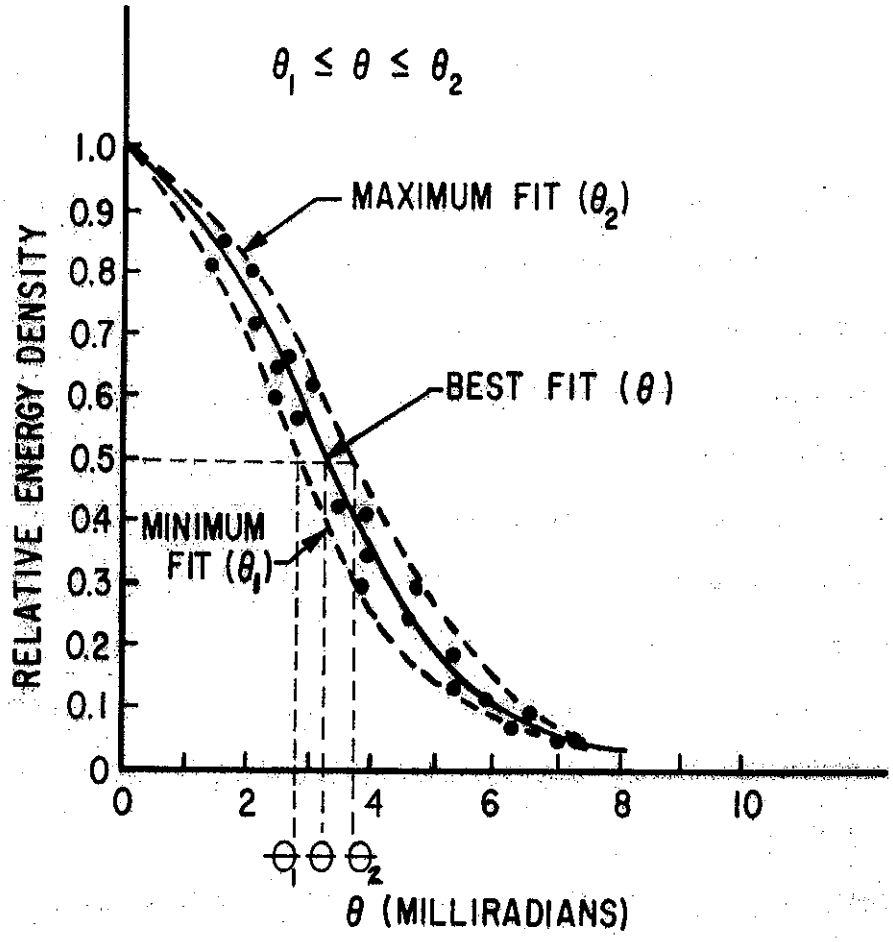

Figure 22. Curve-Fitting Technique For Measuring Beam Divergence